**ADDIS ABABA UNIVERSITY ADDIS ABABA INSTITUTE OF TECHNOLOGY SCHOOL OF MULTIDECIPLINARY ENGINEERING GRADUATE PROGRAM IN RAILWAY ENGINEERING**

# Wear Analysis on Wheel-Rail contact in Rolling-Sliding contact using FEM


**By**

**OUBAH ISMAIL AHMED**


A Thesis`s progress submitted to the School of Graduate Studies of Addis Ababa University in partial fulfillment of the requirements for the Degree of Masters of Science in Railway Mechanical Engineering

**(Railway Stream)**

**Advisor: Dr Daniel Tilahun**

June, 2017

**ADDIS ABABA, ETHIOPIA**

ADDIS ABABA UNIVERSITY

ADDIS ABABA INSTITUTE OF TECHNOLOGY

SCHOOL OF MECHANICAL AND INDUSTRIAL ENGINEERING

Approval of Board of Examining:

| | | |
|---|---|---|
| Name of Chair person, | Signature | Date |
| DR Daniel Tilahun (PHD)<br>Name of Advisor | Signature | Date |
| Name of Internal Examiner | Signature | Date |
| Name of External Examiner | Signature | Date |

ADDIS ABABA UNIVERSITY

ADDIS ABABA INSTITUTE OF TECHNOLOGY

SCHOOL OF MECHANICAL AND INDUSTRIAL ENGINEERING

**DECLARATION**

I, the undersigned, declare "Wear Analysis on Wheel-Rail contact in Rolling-Sliding contact using FEM" is original work of mine and has not been presented for any degree in any university and all the sources of materials used for the thesis have been duly acknowledged.

Oubah Ismail Ahmed ___________________ ___________________

Name Signature

Date

## ABSTRACT

Wheel and rail is one of the most important material used to support and guide rail vehicle safely and smoothly. Since wheel and rail suffers from various interacting mechanical and thermal forces, friction modifiers, various contaminants and environmental atmosphere, wear poses large Problem on wheel and rail.

Wheel and rail wear can be result in an extensive cost for truck owner, if it is not predicated and prevented in an efficient way. To limit these costs, one measure is to predicate and prevent wheel and rail wear through wear modeling.

The purpose of this research is to investigate the wear analysis on wheel / rail in rolling and sliding contact using CATIA V5 R16 software and ANSYS 16.0 Workbench**.** The wear of the wheels has been studies on stress structure as result and the analysis is done for two wheels having different material composition (that is Bainitic steel which is new material and R7 which is using by Ethiopian Light Railway Transit AALRT)

Using stress output as input for structural analysis different stress concentration are observed

The result obtained for the two wheels shows that wheel two has excellent hardness, strength and have good resistance wear

Therefore, Bainitic steel can be applied to wheels in railway system

**ACKNOWLEDGEMENTS**

First of all I would like to thank my advisor Dr. Daniel Tilahun for his grateful support and Continuous advice of the work from the beginning up to the final result of the paper. I want to appreciate also his willingness and giving of motivations to work on research areas focusing on the current situations of the country, Ethiopia, pointing its future development and related problems to lay down the possible respective solutions. I would like to thank also to all people who stand on my side during the work of the paper. Especially to Kenzie Amare and Wudie Dagnew, friends and colleagues who support and guide me during the complex analysis part of wheel/rail contact. Thanks also to engineer Osman who is the mechanical engineer at Ethiopian Railway Corporation and helped me by giving the necessary materials and advice to manage the possible outcomes of the research. Finally, special thanks to my friends Kaltoum and Idil and Roukia for their patience, advice, support and motivation standing always on my side for the successful accomplishment of this paper and for the success of my life at all.

# TABLE OF CONTENTS

# LIST OF FIGURES

# LIST OF TABLES

# NOMENCLATURE

UIC: International union of railways

HCT: Hertz's Contact Theory

AALRT: Addis Ababa Light Railway Transit

Σa : Applied Stress

ΣUTS: Ultimate Tensile Strength of Rail

$R$1w: The Principal Rolling Radii of the Wheel

$R$2w: The principal transverse radii of the wheel

$R$1r: The principal rolling radii of the rail

$R$2r: The principal transverse radii of the rail

a: Major Semi-axis

b: Minor Semi-axis

P: Contact Pressure

Po: Maximum Contact Pressure

$Fn$: The Applied Normal Load at the Wheel/rail Contact

$Kw$: Constants that depend on the material properties of wheel.
$Kr$: Constants that depend on the material properties of rail.

$K3$: Geometrical Properties of both Wheel and Rail.

$vw$ And $Ew$: Poisson's ratio and Young's Modulus of the railway Wheel Material

$vr$ And $Er$: Poisson's ratio and Young's Modulus of railway Rail Material.

M and n: Hertz coefficients

V: Volume of the wear

P: pressure

S: sliding distance

K: coefficient of the wear

H: hardness of the material

# CHAPTER ONE: INTRODUCTION

## 1.1. BACKGROUND

### 1.1.1. HISTORY

The beginning of a new millennium is an appropriate time to review development in railway Technology but the choice of the time period for a review offers some interesting alternatives. Railway technology is old with roots back in the 19th century and more than 170 years of History since opining of a developed form of passenger railway between Liverpool and Manchester. In Principe; the technology today is same as it was in early days; the low friction arrangement Of iron wheels on iron rail but the implementation is vastly different The past 50 years have seen a greater pace of change than any period is perhaps a suitable and Manageable period for review Attempts to improve Railway technology have generally focused on safety and speed important characteristic of rail transport Improving safety and speed is not enough of course; but the focus of Railway development Will probably remain there. However; the social environment in which Railway operate is Evolving meaning that it will become necessary for development of Railway technology to Orient itself in slightly different direction [1].

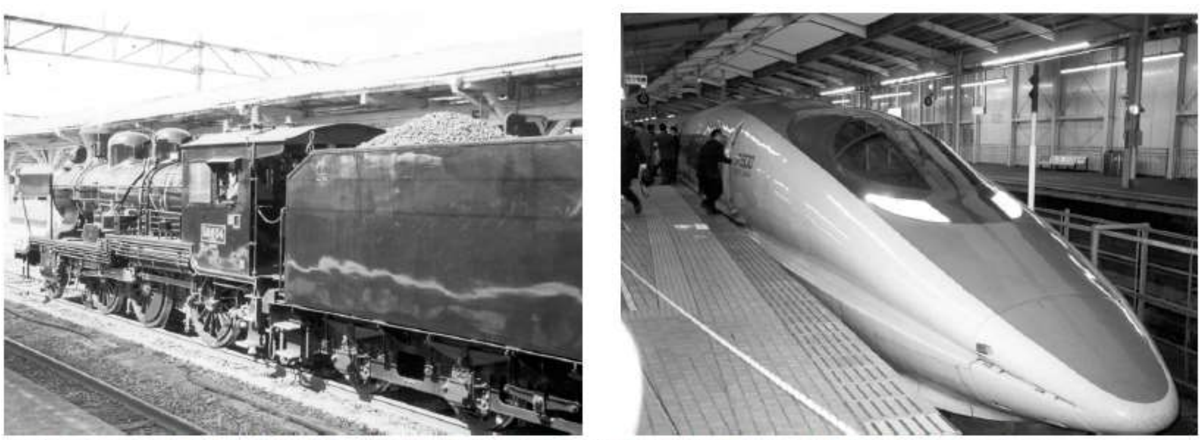

The typical simple mechanical steam engine of 50 years ago has been replaced by the complex mechatronic train exemplified by a Series 500 Shinkansen. (Author)

Figure 1: Comparison between old train and modern train [1].

## 1.1.2. WEAR

Wear is the loss or displacement of material from a contacting surface. Material loss may be in the form of debris. Material displacement may occur by transfer of material from one surface to another by adhesion or by local plastic deformation. There are many different wear mechanisms that can occur between contacting bodies each of them producing different wear rates. The simplest classification of the different types of wear that produce different wear rates is "mild wear" and "severe wear". Mild wear results in a smooth surface that often is smoother than the original surface. On the other hand, severe wear results in a rough surface that often is rougher than the original surface [4]. Mild wear is a form of wear characterized by the removal of materials in very small fragments. Mild wear is favorable in many cases for the wear life of the contact as it causes a smooth run-in of the contacting surfaces. The mechanical action may be sliding, rolling, rolling/sliding or impact motion between worn bodies.

In general wear can be of five types

- **Adhesive wear**: - occurs when the material fragments are pulled off one, initially smooth, N surface and adhere to the other surface in sliding contact. Material is transferred rather than lost.
- **Abrasive wear**: - occurs when rough surfaces slides over one another, displacing material which forms loss wear particle
- **Fatigue wear**: - is observed during repeated sliding or rolling, causing the formation cracks which eventually result in the breakup of surfaces.
- **Corrosive wear**: - occurs when sliding wears break away the protective film formed, allowing further corrosion to take place.
- **Erosive wear**: - occurred due to fluid action on mechanical elements.

In railway wear of wheel and rail occurs due to interaction between wheel and rail. Abrasive wear occurs as a small amount of material removal with every wheel passage. Ratcheting refers to wear mechanism that result of high stress exceeding the elastic limit of the material and leading to some form of plastic flow.

## 1.2. ROLLING AND SLIDING CONTACT

The wheel–rail contact is a rolling–sliding contact. It is easy to imagine wheels rolling on Tracks. On the other hand, wheels will also spin if the tracks are very slippery, for example, if there is ice on the track, in what is known as sliding motion. The combination of the two motions is called rolling–sliding contact. The difference between the circumferential velocity of a driven wheel and the translational velocity of the wheel over the track is usually a non-Zero value, which is known as sliding velocity (*us*). The ratio of sliding velocity to rolling Velocity is called creep or creepage [7] which is the main source of creep force

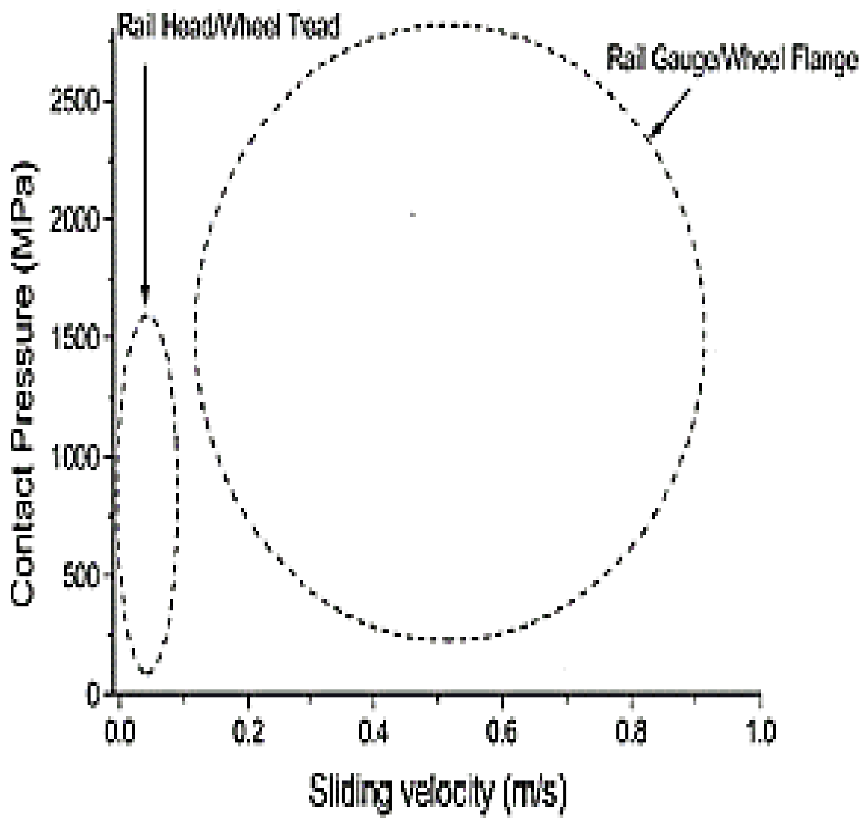


Figure 2: Contact rolling-sliding [7]

## 1.3. STATEMENT OF PROBLEM

One of the basic tasks in study of machine element has traditionally been characterization of wear. Wear defined as the material loss or change in surface textures, occurring when two or three Surfaces of mechanical component contact each other. There are many types of wear and widely varying range of working condition making wear a very complex problem and rail Wear prediction is a current key-topic in the field of railway research. There are different manners to study the wear of the railway where the experimental method is already employed which included twin machine for carry out the higher hardness and field Measurements have been used in the past for study causes of wheel and rail wear. The rolling/sliding wear behavior of wheel or rail can be improved by simulation ANSYS on Wheel or rail. The composition of the material on wheel or rail should be developed and improved. What will happen if we change the compositions of the material on wheel and Rail such as to resist the wear? And how we can choose the performant material? All those Question could be answer and analyses on the time and then this analysis should be compared With the Standard one.

## 1.4. OBJECTVE

### 1.4.1 GENERAL OBJECTIVE

The main objective of this thesis is to analysis wear on wheel-rail contact in rolling and Sliding contact using FEM and the material must be performant for AA LRT

### 1.4.2 SPECIFIC OBJECTIVES

**The specific objective of this research is**

- Study the composition of the material.
- Modeling the material.
- Study the Result of the analysis.
- Compared the Result with the previous experimental Result.

## 1.5. METHODOLOGY OF RESEARCH

The research begins by identifying the determining factors of vertical force  on rail vehicle, raid comfort data were collected and the relationship between those factors have been established to set method to analyze railway raid index. Hence, the following methods were followed.

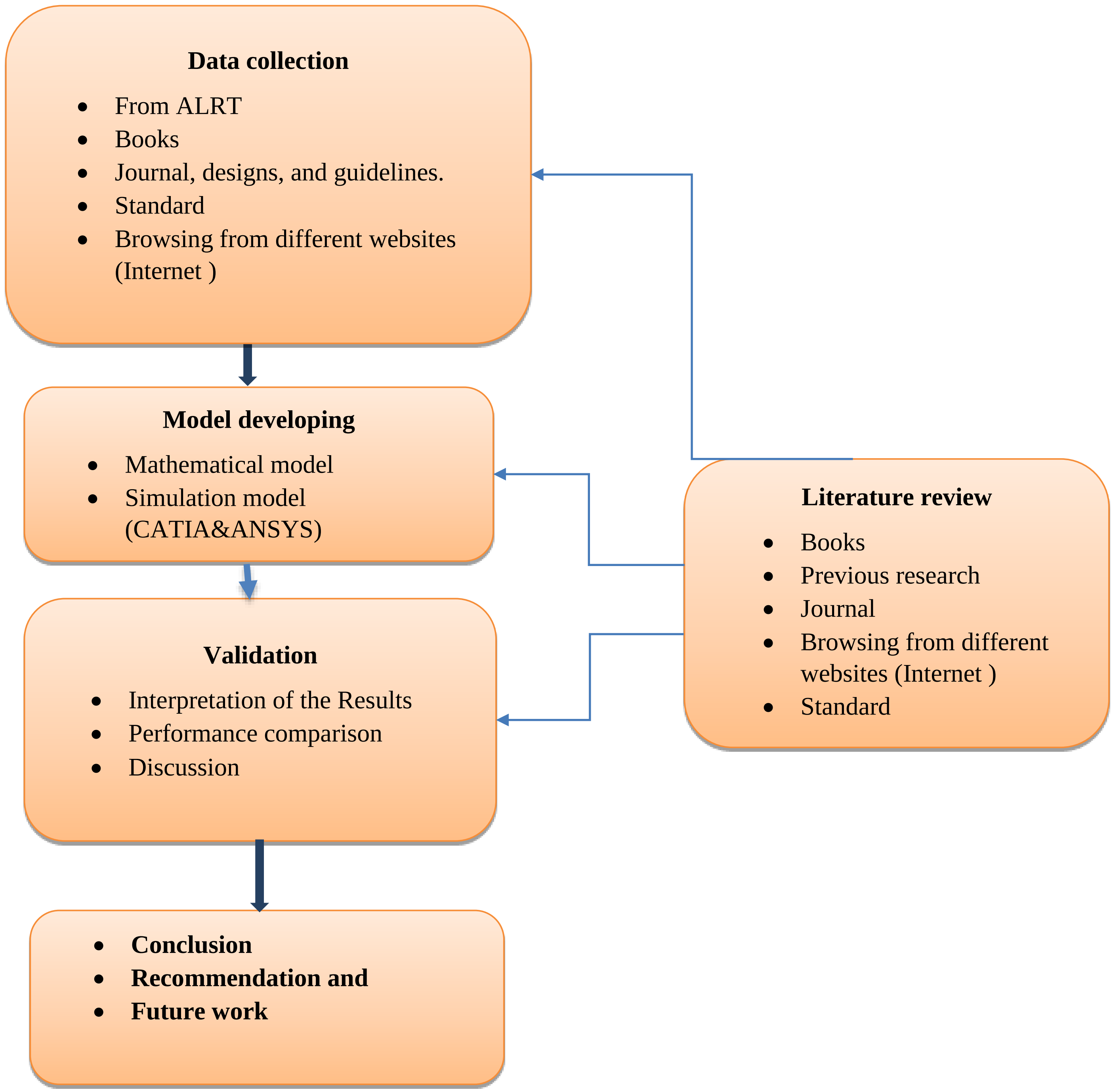


Figure 3: Methodology

## 1.6. SIGNIFICANCE OF THE RESEARCH

This research has most important rule in AA LRT; In order to prevent those repetitive problems happened in Railway such as (Wear; deformation of rail and wheel profile) Those problems have high cost of maintenance and it is first time that my own Country use electric railway for this reason the companies hasn't have enough Information in this case of problem Therefore these researches can help the AA LRT

## 1.7. SCOPE AND LIMITATION

The scope of this research is to carry the analysis wear on Wheel-Rail contact in Rolling and sliding contact the analysis on Wheel-Rail interaction used FEM And this research focus only how to decrease the wear occur between the Contact; for this reason, a material strength enough is required for Railway

**The limitations of the research are following:**

- Stress Analysis on Wheel-Rail contact is not done
- Friction heat on Wheel-Rail contact is not done
- Thermal and mechanical analysis on Wheel-Rail contact is required
- Analysis of corrosive wear due to environmental is required

## 1.8. ORGANIZATION OF THE PAPER

**This thesis paper composed of the following five chapters:**

- **Chapter 1:** Introduction part of the research work including the background, Statement of problem, objective, organization of paper
- **Chapter 2:** Literature review part of the research work including the method, the Material
- **Chapter 3:** Experimental or Analysis method and condition including the Methodology, test rig; condition, dimension
- **Chapter 4:** Discussion and Result at obtained from the simulation will present and discussed
- **Chapter 5:** summarizes the findings in this thesis and draws conclusions which carry to the recommendation and the future work

# CHAPER TWO: LITTERATURE REVIEW

## 2.1. INTRODUCTION

This is one of the portions of the paper that reviews the previous related works which are basic guide for the introduction of the current work. Some of them may have a direct relation with this work whereas the others may have indirect relations. But the main principles they have used and the major methodologies and approaches they precede will be selected generally and applied for the formulation of specific model and analysis. Generally, there are many journals, conference papers, proceedings, design works and books related to the railway engineering, railway vehicle dynamics and particularly wheel rail dynamics, contacts, interactions etc. but to save time and to manage the paper work the review of literatures mainly considers more related works to the paper. This intensifies the deep analysis of the previous related works and selection of appropriate conditions, approaches and methodologies for the successful accomplishment of the paper.

## 2.2. DESCRIPTION OF THE RAILWAY SYSTEM

In railway system, the main function of the track are guiding the train, carrying the loads and distribute the load to a larger area. For instant, a normal load of 10 tones, would create a few square meters [10]. The structure of the track is shown in figure 4 which includes some components such as rails fastening, sleeper, ballast and subgrade

The details of each component are as follows

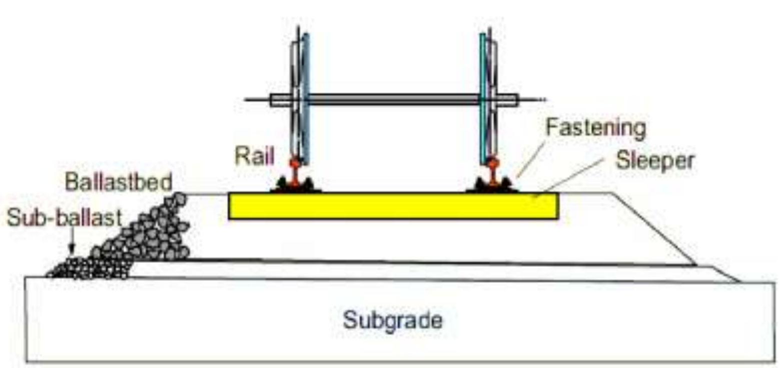


Figure 4: Cross section of the track system [10]

## 2.3. WHEEL WEAR

The life of railway wheels is usually limited by wear [1]. The wheel surface is subjected to high normal and tangential contact stress. Contact forces change their magnitude and orientation when the wheel travels over the rail curves, crossings, and local surface perturbations. The contact is mostly rolling but a small amount of local sliding takes place at the interface. The amount of sliding depends on the contact patch geometry, normal force, lateral force, and friction coefficient. The removal of material from the surface by wear is a function of the sliding and contact stresses [1]. Two main manifestations of wear typically occur on railway wheels: a change in the transversal profile, called regular wear, and the formation of periodic wear patterns in circumferential direction, called wheel out-of-roundness or irregular wear [2]. Regular wear is produced by slow variations of contact forces and creepage associated with the longitudinal and lateral motion of the Wheelset on the track, on straight lines and in curves.

On the other hand, irregular wear is produced by fast variations of wheel-rail contact conditions, which are produced by train-track interaction and are strongly affected by the vertical vibrations of the system. in traction and braking, wear is produced by longitudinal tractive/braking efforts and tends to concentrate on the central portion of the wheel tread, while during curve negotiation the wear process is more complicated, and it involves both longitudinal frictional forces caused by the rolling radius difference between the inner and outer wheels and transversal frictional forces caused by the yaw angle of the wheelset [3, 4]. As a consequence of this complex wheel-rail contact condition, two distinct wear regions appear on the wheel profile: one on the flange and the other the thread

Wear rates in these two regions depend on different factors, such as the vehicle design, the service profile, the status of the contacting surfaces (including the possible presence of natural or artificial lubrication) and the mechanical properties of wheel and rail materials

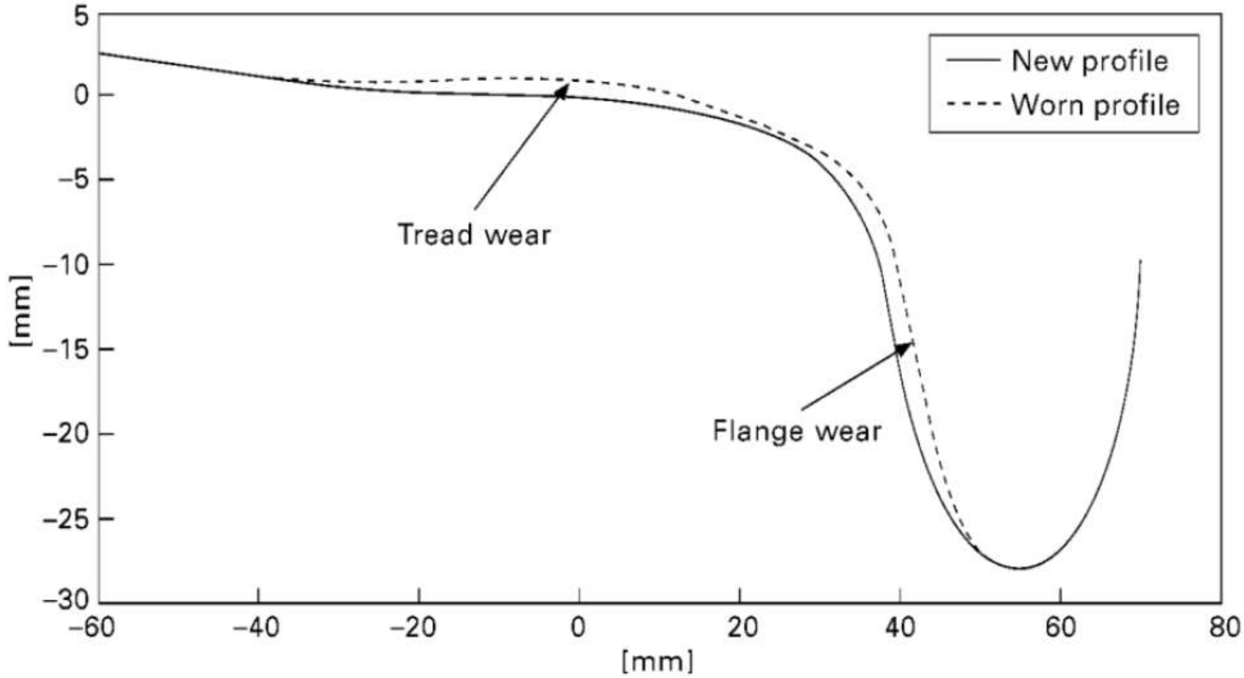


Figure 5: Wear regions on the wheel profile. [16]

## 2.4. WHEEL-RAIL CONTACT

There are several publications available which are concerned with wheel–rail contact. Various methods, results and measurements were published. Kleiner and Schindler [46] used FE analyses to determine the pressure distribution between the two contacting bodies. Their analyses involve 17 contact positions between an S1002 wheel profile and a 60E2 rail profile. In addition, an empirical equation was established which makes it possible to determine – with a good approximation – the Maximum surface pressure depending on the wheel load and the lateral displacement of the wheel relative to the rail. The normal pressure distribution on the surface of the tread in different lateral contact positions. Similarly, to the contact stress, the equivalent stress distribution on and under both surfaces of the wheel tread and the rail was examined. Furthermore, they investigated the stress distributions in the case of a driving-wheel. Besides Kleiner and Schindler, a great number of other researchers such as Sladkowski and Sitarz [46], Arslan and Kayabaşi [47] and Aalami et al. [48] applied FEM with 3D models to investigate the contact zone(s) and stresses in the wheel-rail contact during stationary and rolling conditions

A)

B)

Figure 6: Front views (A), and side view (B) of wheel/rail contact interface [46]

## 2.5. WHEEL AND RAIL WEAR

The wear that inevitably occurs between the wheel and the rail while the vehicle is moving depends on a large number of factors, among which sliding phenomena inside the contact patch, the normal force transmitted, the friction coefficient, lubrication conditions, size and shape of the contact patch etc. Wear on wheels and rails makes it necessary for equipment to be replaced when the upper safety limits have been reached and, as a general rule, the vehicle also sustains losses in terms of dynamic performance. Worn profiles tend to be less stable and show lower performance levels when negotiating curved tracks, and this makes reducing the wear index a major factor in the design of railway vehicles [39].

Traditionally, the wear of materials has been characterized by weight loss and wear rate. However,

Studies have found that wear coefficient is more suitable [40].

The reason being that it takes the wear rate, the applied load, and the hardness of the wear pin into

Account. Although, measurement variations by an order of 10-1 have been observed, the

Variations can be minimized if suitable Precautions are taken.

A wear volume versus distance curve can be divided into at least two regimes, the transient wear regime and the steady-state wear regime. The volume or weight loss is initially curvilinear. The wear rate per unit sliding distance in the transient wear regime decreases until it has reached a constant value in the steady-state wear regime. Hence the standard wear coefficient value obtained from a volume loss versus distance curve is a function of the sliding distance

Table 1: K values for various materials

| **Materials** | **K** |
|---|---|
| Mild steel (on mild steel) | $7\times10^{-3}$ |
| α- / β-brass | $6\times10^{-4}$ |
| PTFE | $2.5\times10^{-5}$ |
| Copper-beryllium | $3.7\times10^{-5}$ |
| Hard tool steel | $1.3\times10^{-4}$ |
| Ferritic stainless steel | $1.7\times10^{-5}$ |
| Polythene | $1.3\times10^{-7}$ |
| PMMA | $7\times10^{-6}$ |

## 2.6. DEFECTS OF RAILWAY WHEELS

The defects of the railway wheels can be classified into the following major groups according to [43]:

- ***Thermal cracks:***

The most severe type of wheel defects. Thermal cracks occur as a result of the alternate heating and cooling process of the wheel tread and partly the rim under braking. The cracks are caused by metallurgical changes in the wheel material. In most cases, thermal cracks are located transversally on the wheel tread and can be removed by machining. Without preventive action, thermal cracks can reach the point when the wheel will fracture. Typical thermal cracks on the wheel can be seen in Figure 8 [43].

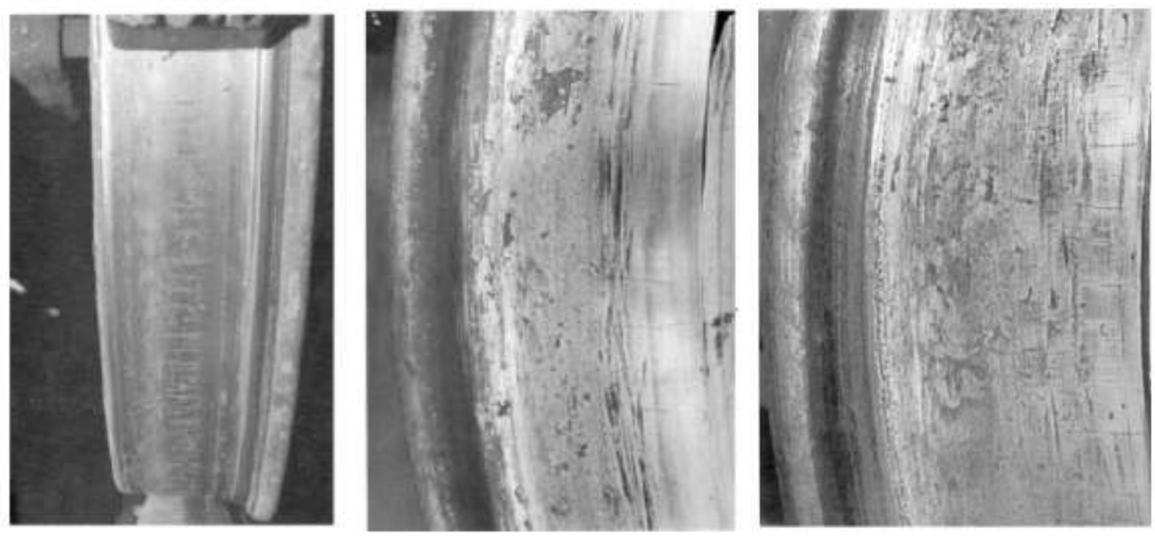

b) c)

Figure 8: Different classes of thermal cracks on the wheel tread [43]

a) Claas 2 thermal crack; b) Claas 3 thermal crack; c) Claas 4 thermal crack

- ***Contact Fatigue:***

These defects are the results of repeated contact stress during rolling motion. They are located On the wheel tread surface and not oriented perpendicularly to the running direction (chevron Type indication). Spalling is usually caused by rolling fatigue cracks. Rolling contact fatigue Cracks can be seen in Figure 9 [43], [44]

Figure 9: Rolling fatigue cracks on the tread [44]

- ***Fatigue cracks***

These defects are caused by either external damage or a manufacturing fault. They usually appear as solitary cracks. A fatigue crack can be seen in Figure 10 [43].

Figure 10: Fatigue crack on the tread propagated from thermal crack [43]

- ***Damaged wheels***

This group consists of manufacturing defects, out-of-round wheels and overheated wheels. In the case of manufacturing defects, the failure that has occurred on the wheel web can result in a fatigue crack which propagates circumferentially around the web. An out-of-round wheel is another form of manufacturing defect. In this case, the wheel tread was turned out-of-round, e.g. the milling cutter was not fed correctly or the wheel tread was not turned concentrically to the axle Centre. Damage caused to the wheel by a heavy external impact is called an external wheel damage. This external impact may cause fatigue cracks to start and propagate quickly through the entire wheel. Figure 11 show different manufacturing defects [43].

Figure 11: Incorrect mill feed as a result of bad turning [43]

## 2.7. RAIL

### 2.7.1. RAIL NOMENCLATURES AND PROFILE

Before discussing about rail, it is necessary to have some understanding of the terminology that is commonly used with rails. Some of the rail terminologies are discussed as follows [35, 36].

- **Running Surface** - zone on top of the rail head, which makes contact with wheel tread.
- **Gauge Corner Region** - top corner on the gauge side of the rail, which makes contact with the wheel throat region
- **Field Corner Region** - top corner on the field side of the rail
- **Fishing Surface** - the region at the bottom of the rail head, which makes contact with fish plates
- **Rail Head** - The region of the rail that is above the extensions of the fishing surfaces to the rail Centre line
- **Rail Foot** - the region of the rail that is below the extensions of the top of foot surfaces to the rail Centre line.
- **Rail Web** - the region of the rail that is between the rail head and the rail foot

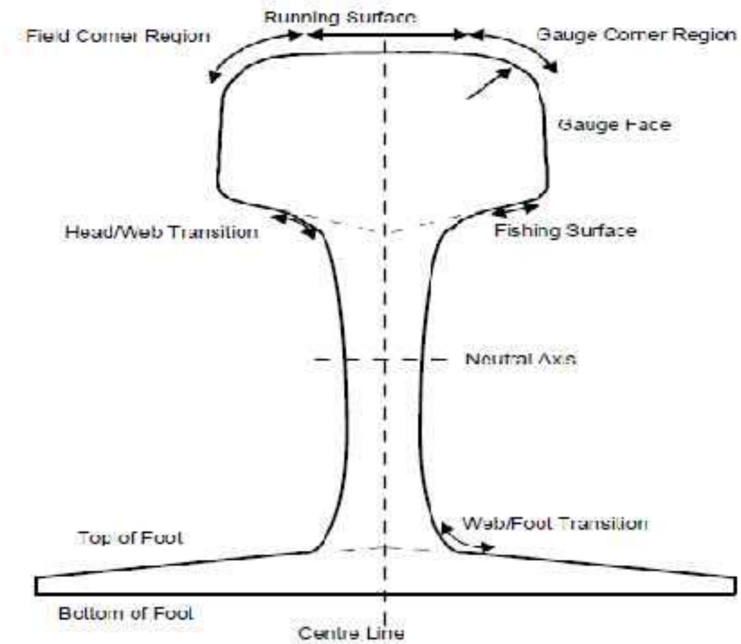


Figure 12: Terminologies used with rail [35]

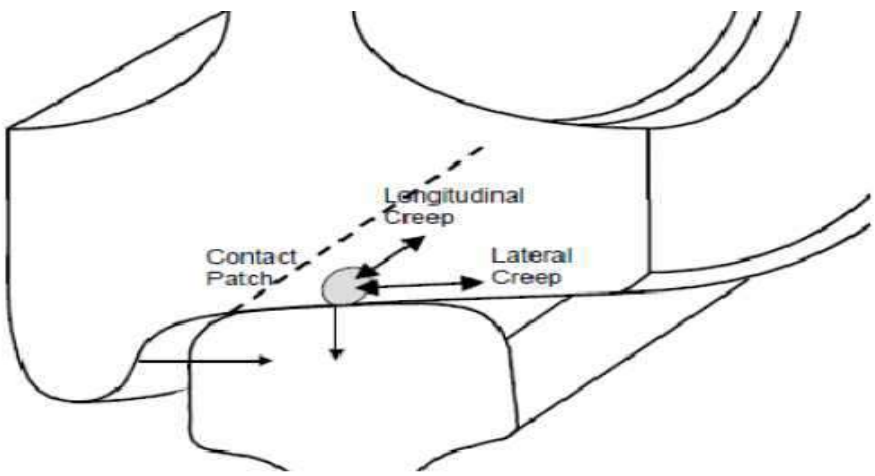


Figure 13**:** Terminologies used for wheel/rail loads [36]

Rail can be classified into two by considering its profile. These are simple wide foot rail and Special groove rail. These two types of rails have similar foot, but different rail head. Rail type can be named according to its weight per meter length (kg/m) [38]. The higher the weight, the higher the load it can take, and thus adapts to heavier train. Rail types are specified in UIC, EN specifications [37].

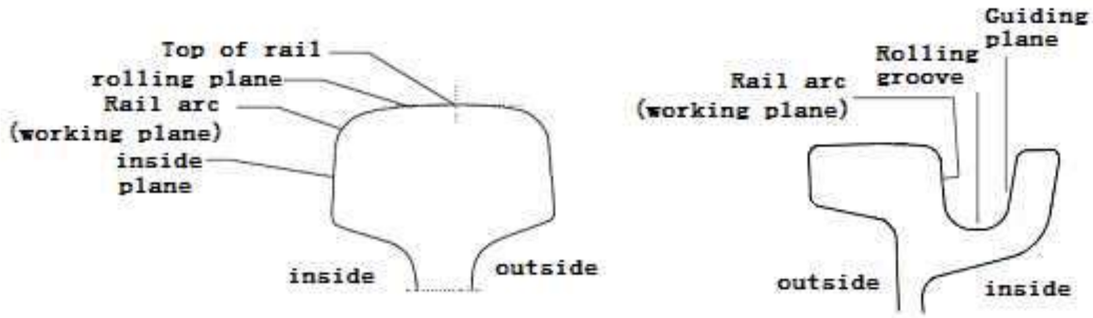


Figure 14: Rail head profile and its definition [37]

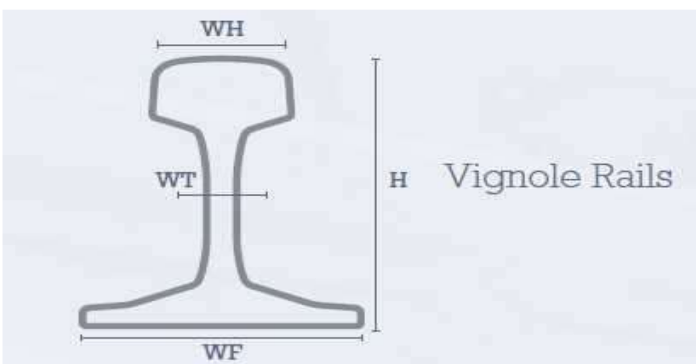


Figure 15: Rail dimensions and definitions [38]

Since the rail/wheel contact is in fact rather an elliptical than a line contact, the radius *R* and the normal load *P* for the cylinder model are chosen in the way that the maximum Hertzian pressure pH of the smooth two-dimensional case equals the one of the three-dimensional case, and the Hertzian half-length *a* H equals the length of the radius *a* of the contact ellipse in rolling direction (Fig. 6). The influence on the calculated area of contact of two basic characteristics of the surface topographies are systematically evaluated. The first one is the distribution of the height values in *z*-direction. Therefore, the standard roughness parameters, *R*a and $\sigma$ (= *Rq*), are considered. The second characteristic is the spatial distribution of the heights in *x*-direction. The simulations are performed for the same nominal surface profiles, but different low-pass filter frequencies for the profile data. One side effect, which has to be taken into account is the slight decrease in the roughness parameters *R*a and $\sigma$ with decreasing filter frequency. If not particularly mentioned, the roughness parameters of a certain profile given in this work refer to the original unfiltered data

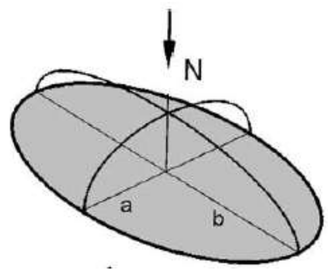


Figure 16: Three dimension of the Wheel-Rail contact

R7 is by far the most commonly used grade [49]. It is used for all freight wagon wheels and on most passenger's coaches where wheels made from R7 are intended for use in vehicle with tread brakes, the value. Experience shown that where carbon content exceeds 0.5%, the Kic values of 80MPa and high homogeneity are present in the microstructure throughout the circumference of the wheel. This supplied with lower carbon content (0.5% C) which therefore puts them often in the lower strength tolerance range, so that beside pearlite, large amount of pre-eutectoid ferrite is present in the tread.

Although this leads to greater toughness, the wear resistance is correspondingly diminishing. According to DB experience, free (pre-eutectoid) ferrite content of < 10% is advantageous in term OD minimizing wheel wear at the tread, for driven wheels on locomotives and motor coaches, R8 is increasingly the used grade, R9 is limited to niche application permanent way construction vehicle and combined transport system such as the Rolling Road **[11]:** Contact is the principal method of applying loads between deformable solids, and Therefore is present in a wide variety of mechanical components. In addition, contacts usually act as stress concentrations, and are thus probable locations for mechanical failure. Some of the most typical mechanical failures involving contact include: fretting, fretting fatigue, wear, fretting wear and false brinelling. The contact of UIC-60 and IRS-T12 rail-wheel has been analyzed by hand calculations to determine contact stresses. A three-dimensional finite element model of both type of rail-wheel contact is developed in ANSYS to compare to the typical hand calculated stresses. A vertical force is applied railway wheel & simulates the effects frictional surfaces. The results of the finite element model analysis contained herein are compared to hand calculations. Based on these results, a finite element analysis should be used if a greater level of detail is required for the analysis of the rail-wheel contact.

- IRS-T12 rail-wheel are less than UIC-60 rail-wheel which shows suitability of IRST12rail-wheel on the basis of strength.
- IRS-T12 rail-wheel is having higher corrosion resistance and more life than UIC-60 Rail-wheel
- IRS-T12 rail-wheel is having less failure chances as compared to UIC-60 rail wheel Due to less contact stresses developed **[6]:**

Rail transport is one of the most important branches of economics activity of which is directed at support of internal and external transport relations [Myamlin 2006]. Safety of train operation depends much on reliable functioning of the assemblies and transport means. It is ensured by stable and optimal level of metal mechanical properties, as well as soundness of metal. Required level of mechanical properties of assemblies and components is provided by chemical composition of steel and structure after thermal treatment. Locomotive wheel pairs take and transfer weight of body and bogies with all equipment on rails, as well as dead weight. While moving wheel pair interacts with rail gauge, takes up shocks caused by track irregularities and guiding forces. Wheel pair, in its turn, rigidly reacts on track. In addition, traction motor torque is transmitted to it, tractive and braking forces are realized in place of contact of wheels with rails. Magnitude and nature of effect of static and dynamic forces depend on conditions of operation and rail track state, design and parameters of locomotive underframe. Thus, wheel pair is one of critical assemblies of underframe on state of which train operation safety depends. Therefore, special demands are made to the material choice, manufacturing of separate elements and formation of wheel pair [Filonov 1996]. Taking into account complicated working conditions and high requirements to the operational dependability, wheel tread surface should possess high strength, impact toughness and wear resistance, whereas metal of wheel disk and hub is to have required toughness. Compound wheels meet these requirements, where tyre can be made of high strength and dead-hard steel, whereas wheel center – of more ductile and cheap steel.

Upon reaching limiting wear or appearing of another operational damage a tyre can be replaced without change of a wheel [Lukin 2000]. Tyres directly interact with rails. Main characteristics of tyres defining their quality and service durability are strength and hardness of tyre body and flange. The higher strength and hardness are, the higher wear resistance is. Therefore, tyre material should possess high strength to resist wear and crumpling, and should be tough enough to resist impact loads [Filonov 1996]. During locomotive operation tyre wear occurs over wheel rolling circle. So, the metal earlier contained inside the tyre will appear on the surface of the used tyre, and this metal will work in conditions of contact with rails and brake shoes. That’s why metal in sectional view must meet technical requirements of normative documents. At present tyres are produced for railway rolling stock in accordance with standards. Tyres are manufactured of 2 grade steel for passenger, freight and shunting locomotives, driving motor cars, diesel-powered trains and transit vehicles. Chemical composition is specified in table 2.

Table 2: Chemical composition of tyres (metal steel) made of 2 grade steels [7]

| Content of elements, % by weight | | | | | |
|---|---|---|---|---|---|
| C | Si | Mn | V | P | S |
| | | | | not more than | |
| 0.57-0.65 | 0.22-0.45 | 0.60-0.90 | up to 0.15 | 0.035 | 0.040 |

Total content of sulfur and phosphorus must not exceed 0.065%. Permissible content of molybdenum is not more than 0.08%, nickel – not more than 0.25%, chromium – not more than 0.20%, copper – not more than 0.30%. One of the evaluation parameters for metal properties is Brinell hardness. Hardness is measured by a sphere 10mm at a load 29430N on a transverse template on the basis of mean value of three measurements at a depth 20mm and three measurements at a depth 40mm from a tread surface. Hardness measurement is fulfilled on the flange in one point. While manufacturing high speed railway rolling stock and for the purpose of providing safe operation on the railways there appeared a task to improve ultrasonic nondestructive test of wheel pair elements. Metal inhomogeneity (inhomogeneity of chemical composition, structure) exerts influence on the quality of ultrasonic control. It influences stability of acoustic properties, first of all of acoustic vibration speed, damping coefficient, it results in an uneven sensitivity, and errors of defect coordinate measuring. [9]: The aim of the present paper is to study inelastic processes (plastic deformation and fracture) in this sub micrometer ranges and to determine the friction forces resulting from these inelastic processes in our case, a modeled object consisted of four parts:

. The upper layer of automata was an absolutely rigid, non-deformable body moving horizontally at velocities v ranging between 1 and 10 m/s in different numerical experiments;

. Two intermediate layers with initial roughness of nanometer range represented surface regions of the bodies in contact;

. The lower layer was a fixed support. A constant normal force corresponding to the pressure

Range between P = 0.5 Mpa and P = 26 Mpa acted upon all the elements of the upper layer. The diameter of the automata was from 2.5 to 10 nm in different numerical experiments.

The elastic properties of the automata corresponded to the steel with Young's modulus of E = 206 GPA and Poisson.s ratio of n = 0.3. The yield strength y1 s and ultimate strength

With respect to tension s0 were varied between 80 and 480 MPa and between 92 and 552 MPa, respectively. An important parameter determining stability of the plastic deformation processes and significantly affecting the characteristic size of the surface region of the severe plastic deformation is viscosity. Introduction of viscosity is necessary already from a formal consideration of providing stability to the calculation procedure. Phenomenological viscosity Reflects dissipation processes under strain occurring due to electron and phonon excitation in a solid. It was assumed in the numerical model that viscous forces acting between unconnected but contacting automata are proportional to the relative velocity of motion. At the left and right fragment boundaries, periodic boundary conditions were used. The initial roughness was specified in the explicit form the material parameters used are listed in table 2 [32]:

Laboratory testing of two types of Duroc laser-cladded rail steel was carried out at the University of Sheffield on the SUROS twin disc test machine (described in detail by Fletcher and beyond [32].

The outer diameter (i.e., the running surface – see Figure 4) of the specimens was 47.3mm, and the coating thickness on the rail discs was typically 0.6-0.7mm. The base material of the rail disc specimens was cut from a UIC 900A rail, while the wheel disc material was cut from a B5T wheel. Figure 4, test disc specifications (dimensions in mm). Of the two coatings tested, one was marked Duroc 508, the second Duroc 222. Both proved to have excellent rolling contact fatigue and wear resistance under wet conditions with a Hertzian peak contact pressure of 1.5GPa (an applied load of approximately 7.18kN) at –1% slip. These experiments started with 1,000 dry cycles, a technique normally useful for initiating cracks which would subsequently be propagated, followed in one case by 20,000 wet cycles and in another case by 200,000 wet cycles. The lubricant was distilled water and applied at the rate of two drips per second. In each case the eddy current probe detected no signs of cracking of the rail disc. A similar experiment carried out on an uncoated rail

Disc resulted in a gate triggering crack after 1,000 dry cycles and a mere 3,000 wet cycles. Traction coefficient was measured for the duration of each test (see Figure 5). In the reference test with the uncoated rail disc, the traction coefficient rose to 0.44 during dry cycling, and steadied at 0.21 during wet cycling. The dry traction coefficient for the 508 coating was 0.42-0.43, effectively the same as for the uncoated specimen, while the traction coefficient during dry cycling for the 222 materials was 0.39. However, traction behavior during wet cycling was markedly different for the two materials. During the first 40,000 wet cycles of the long duration test with the 508- coating, the traction coefficient rose to a maximum of 0.33, accompanied by rusting of the surface; subsequently it dropped gradually, accompanied by de-rusting of the surface, reaching 0.21 after 200,000 cycles. With the 222-coating, on the other hand, the traction coefficient peaks at 0.30-0.32 after 5,000-7,000 wet cycles, but steadies at 0.16 by 20,000 cycles. Therefore, in both dry and wet cycling, the 222-coating showed the lower coefficient of traction of the tested samples.

Table 3: Steel material [9]

| Parameters of a model material | |
|---|---|
| Young modulus | E= 206 Gpa |
| Poisson radio | V= 0.3 |
| Density | P= 7800 kg/m³ |
| Elastic limit | θy1= 51-306 Mpa |
| Yield stress | θy2= 80-481 Mpa |
| Strain yield stress | Ɛy2= 0.015 |
| Tensile strength | Θ= 92-552 Mpa |
| Fracture deformation | Ɛ= 0.04 |
| Viscosity | Ŋ= 0.41pas |

**[44]:** The idea behind the development of new steel grade called articlos for manufactures of Railway solid wheels was to take a steel grade likes ER7, ER8 with all good toughness characteristic and combine it with higher and strength of ER9 steel grade The new steel is designed to guarantee wheel resistance against wear and particular rolling contact fatigue (RCF), the new steel grade is undergoing both standards Europeans test for new wheels and special test according to Russian Gost standards, while the application of so-called quality maps, which is standards for luchini RS steel production process assures the safety and performance of material The use of quality indices not only allows a comparisons of performance of different qualities but also shows the improvement of each steel grade in sample graph

DB System technic has for years been investigating operationally induced flaws to rails and Wheels in order to arrive at means of slowing down or actually preventing damage processes. One option here is to use rail materials of greater strength that accordingly have a higher resistance to rolling contact fatigue (RCF) [51]. Over recent years, DB System technic has been investigating the suitability of pearlitic and bainitic rail steels for use on lines with rolling contact fatigue problems with the aim of cutting track maintenance input without increasing the level of vehicle maintenance due to increased wheel wear. The present findings indicate that, as well as reducing wear, higher-strength pearlite grades also result in shallower head checks, enabling them to at least delay the attendant damage done to the rail. Furthermore, with suitable alloying and control of the form that sapphires take, non-heat-treated, naturally hard steels could well be developed as an alternative to the head-hardened rail, especially since the wear at weld joints to which head-hardened rails are subject would cease to exist. Bainitic rail steels may produce a balance between the processes of wear and rolling contact fatigue at a low level. However, minimum strengths need to be observed when using them, though, due to the altered wear mechanisms of pearlite steels. The present findings indicate that high-chromium steels with a medium carbon content and hence of considerably greater strength deliver better wear behavior than high-manganese steels with a low carbon content.

This paper reviews and critically discusses different methods suitable to data analyses of sliding wear tests and proposes new approaches [33]. The Archard's wear equation was revisited and re-arranged in order to introduce the friction force instead of the normal load, resulting in a substantiation of the energetic approach of sliding wear. Analyzing the results of the brass/hard steel sliding pair, it was demonstrated that the method used to analyses the results plays an important role in the scatter of specific wear rate values. As the majority of sliding tests reveal the existence of a first step where the wear is not linear with time, the assumption of a constant wear rate during the entire test could be a rough approximation. The energetic approach is a promising alternative method to characterise the wear behavior of engineering materials.

Based on experiments Archard [33] achieved the following conclusions:

- The material volume removed by wear is proportional to the sliding distance;
- The material volume removed by wear is proportional to the normal applied load;
- The materials display a wear amount inversely proportional to their hardness.

Considering the above conditions, the widely known Archard's equation can be easily established, equation (1).

$$V = K \frac{NX}{H}$$

Where *V* is the wear volume, *N* is the normal load, *x* is the sliding distance, *H* is the hardness of the material and *K* is a non-dimensional wear coefficient.

# CHAPTER THREE: ANALYTICAL METHOD AND CONDITION

## 3.1. INTRODUCTION

To obtain accurate solutions of the wheel/rail contact problem there are different steps and procedures to be employed. The calculation of wheel-rail contact forces in the dynamic simulation of railroad vehicles involves the following steps [2]:

1. Location of the position of the contact points on the surfaces of the wheel and rail.
2. Calculation of the normal contact forces.
3. Calculation of the Wear rate between Wheel-Rail Contact

It is important that the wheel wear process can be modeled, as this enables improvements to be made to wheel design and materials in order to keep wear at a minimum. Excessive wear needs to be avoided as this can affect the dynamic behavior of the railway vehicles, which will reduce the ride comfort, augment the cost for maintenance and replacement of wheels, increase the vehicle-track interaction forces that may have an impact upon the potential for derailment, and reduce the integrity of the wheel material [2]. There will also be negative effects on the track, increasing maintenance cost of rails and the infrastructure. Understanding of the wear rates will also help with planning regrinding schedules.

## 3.2. DIMENSION

Vehicles that operate on Rail Tracks shall be designed and maintained so that the geometric features of wheels and Rail are compatible with those of Railway Track, to sustain safe operation vehicles under all normal condition on those routes where they are permitted

Addis Ababa Light Railway Train cars has a wheel diameter dimension 630mm and the web structure is called-web [**Ethiopian Railway Corporation, technical specification of vehicle]**

## 3.2.1. MAIN DIMENSIONS OF WHEEL AND RAIL

The principal rolling radii of the wheel: $R1w = 330$ mm

The principal transverse radii of the wheel: $R2w = \infty$

The principal rolling radii of the rail: $R1r = \infty$

The principal transverse radii of the rail: $R2r = 300$ mm

**(Source: Ethiopian Railway Corporation, technical specification of vehicle)**

Table 4: Component material and dimension

| Part name | Standard | Material | Dimension |
|---|---|---|---|
| wheel 1 | UIC60 | R7 | Dia= 660mm |
| wheel 2 | __ | low-medium carbon steel | Dia= 660mm |
| Rail | UIC60 | UIC50 | Length= 25m |

### 3.1.1 DIMENSION OF RAIL

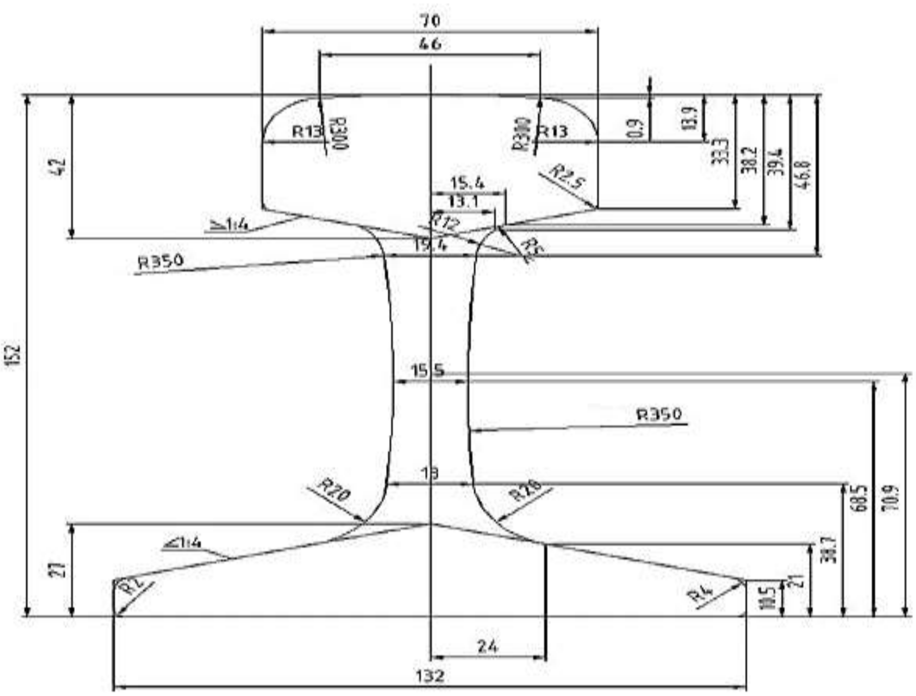


FIGURE 17: Dimension of the Standard rail

**(Source: Ethiopian Railway Corporation, technical specification of vehicle)**

### 3.1.2 DIMENSION OF WHEEL

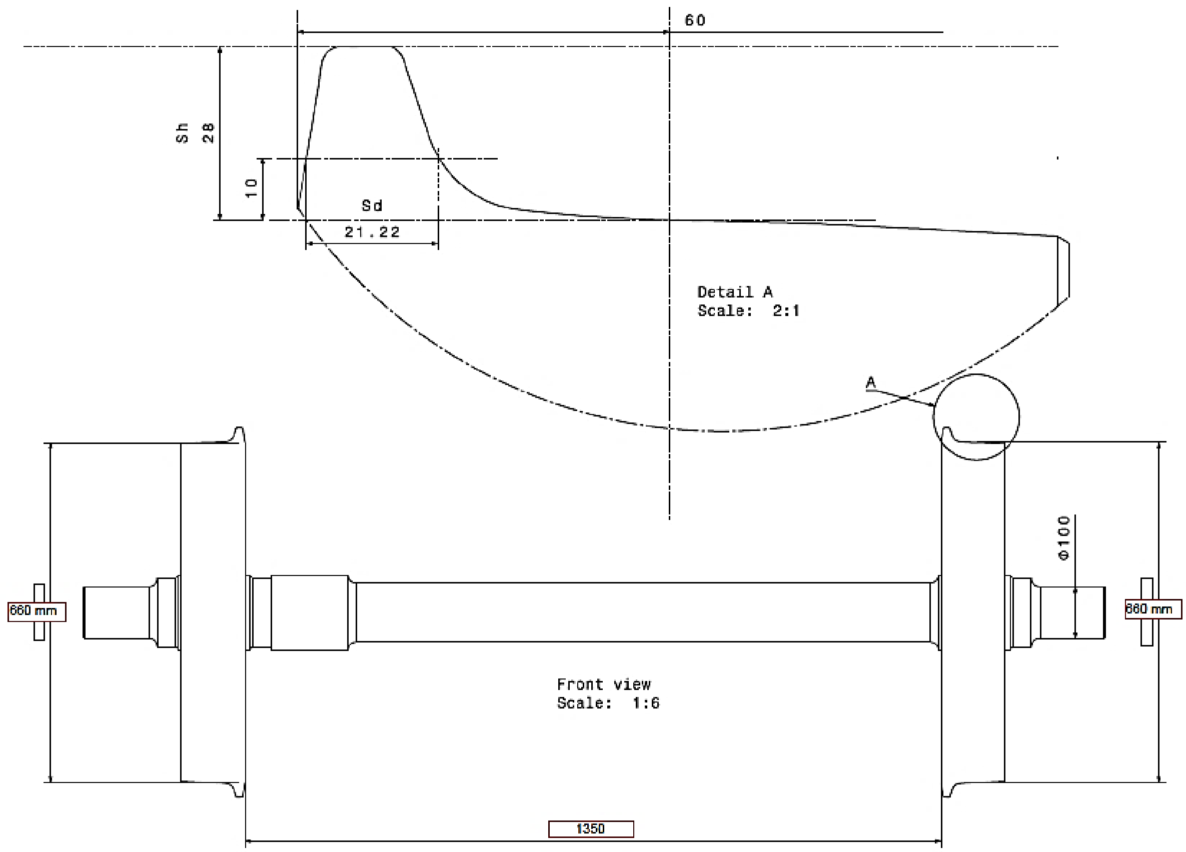


FIGURE 18: Dimension of the standard wheel

**(Source: Ethiopian Railway Corporation, technical specification of vehicle)**

## 3.3. MATERIAL

The common and inexpensive metal, steel has one of the highest values of elastic modulus, for this reason and because steel is relatively inexpensive and offers a very attractive combination of strength, ductility, wear resistance almost all wheels and Rail worldwide are made from plain carbon-manganese steel, which has a lamellar structure of iron and iron carbide

Railway wheels are the key parts that must have better quality to Wear resistance, Thermal crack, Fatigue and fracture leading to a sudden catastrophic failure. In the present time, the wheels are made of high carbon grade steel

Wheel 1 (R7) is typically wheel steel with carbon content (0.5%) which therefore puts them often in lower strength tolerance range so that leader to greater toughness.

The chemical composition of Wheel 1and Wheel 2 are shown in Table 5 and 7, the banite steel is low-medium carbon Si-Mn-Mo-V steel with sufficient silicon to prevent the precipitation of carbide during phase transformation at slow cooling rate and sufficient manganese for purpose of increasing hardenability and some other alloy such as molybdenum and vanadium . The addition of molybdenum and vanadium facilitate to achieve the desired hardenability for obtaining uniform hardness and beneficial for achieving higher tensile strength and toughness

Table 5: Chemical composition of R7 wheel material [50]

| Chemical element | C | Si | Mn | P | S | Cr | Cu | Mo | Ni | V | Cr+Mo+Ni |
|---|---|---|---|---|---|---|---|---|---|---|---|
| Amount (%) | 0.52 | 0.4 | 0.8 | 0.4 | 0.4 | 0.3 | 0.3 | 0.08 | 0.3 | 0.05 | 0.6 |

Table 6: Mechanical properties of R7 wheel (wheel 1) material [50]

| | |
|---|---|
| **Yield strength(MPA)** | **540** |
| **ultimate tensile strength(MPA)** | **820** |
| **Hardness (HB)** | **241** |
| **Elongation (%)** | **14** |
| **Modulus elasticity(GPA)** | **210** |

Table 7: Chemical properties of Bainitic wheel (wheel 2) material [17]

| **Chemical element** | **C** | **Si** | **Mn** | **Mo** | **V** | **S** | **P** | **Cr** | **Ni** | **Cu** | **Fe** |
|---|---|---|---|---|---|---|---|---|---|---|---|
| **Amount (%)** | **0.19** | **1.44** | **1.87** | **0.26** | **0.07** | **0.004** | **0.013** | **0.09** | **0.22** | **0.03** | **Bal** |

Table 8: Mechanical properties of Bainitic wheel material [17]

| | |
|---|---|
| **Yield strength(MPA)** | **560** |
| **Ultimate tensile strength (MPA)** | **1090** |
| **Hardness (HB)** | **273** |
| **Elongation** | **15** |
| **Modulus elasticity(GPA)** | **210** |
| **Poison ratio** | **0.3** |

Table 9: chemical properties of UIC50 Rail material

| Material | C (%) | Si (%) | Mn (%) | P (%) | S (%) | Ni (%) | Cr (%) |
|---|---|---|---|---|---|---|---|
| Rail | 0.8 | 0.28 | 1 | 0.04 max | 0.05 max | __ | __ |

Table 10: Mechanical properties of UIC50 Rail material

| | |
|---|---|
| Yield strength (MPA) | 540 |
| Elongation (%) | ≥10 |
| Ultimate tensile strength (GPA) | 780 |
| Poison ratio | 0.3 |
| Young s Modulus (GPA) | 207 |
| Density (kg/ m³) | 7800 |

**(Source: Ethiopian Railway Corporation, technical specification of vehicle)**

## 3.4. CONDITIONS

The below tables show that the general technical parameters and condition of freight car of the national Railway of Ethiopia [Source: Railways corporation, rolling stocks specifications]

Table 11: Technical parameters of passenger car for Addis Ababa Light Railway Transit

| Technical Values | Values | Units |
|---|---|---|
| Railway Gauge | 1435 | Mm |
| loading capacity | 70 | Kg |
| Wheel Diameter | 600 | Mm |
| max speed | 70 | Km /H |
| axle load | ≤11（1+3%） | Tones |
| Minimum radius of vertical curve | 1000 | M |
| Maximum gradient | 55 | % |
| Empty vehicle load | 44 | Tones |
| Type of rails for main lines and depot | 50 | kg/m |

**(Source: Ethiopian Railway Corporation, technical specification of vehicle)**

Table 12: Geometrical dimension and application parameters

| | |
|---|---|
| **Axle load (ton)** | **≤11（1+3%）tone’s** |
| **Maximum speed(Km/h)** | **70Km/h** |
| **Radius of wheel(mm)** | **300mm** |
| **Ambient temperature** | **25˚C** |

**Natural Environment in Addis Ababa Region**

| | |
|---|---|
| Altitude: | ≤2500m |
| Ambient temperature: | 0℃～+29.7℃ |
| Average daily highest temperature in years: | 25.5℃ |
| Average daily lowest temperature in years: | 6.1℃ |
| Average relative humidity in year | 95% |
| Average annual rain fall: | 1000-1600mm |
| Maximum daily rain fall: | 47mm |

## 3.5. COST OF WHEEL & RAIL

Table 13: Cost of the wheel-rail material

| **Diameter** | **Place of origin** | **Material** | **Price/ pieces** |
|---|---|---|---|
| **650mm-780mm-840mm-920mm** | Qingdao, Shanghai, Shenzhen and other China ports | ER6, ER7, ER8, ER9, R7T, R8T, R9T, CL60, Bainitic, U71Mn, U75V | US $500-1000 depend on their diamters |

## 3.6. WHEEL/RAIL ANALYSIS METHODS

From elementary mechanics, it is known that two contact surfaces under load will deform. Depending on the magnitude of the load applied and the materials' hardness, the deformation may be either plastic or elastic. For many engineering applications, the contact surfaces are non-conformal. The resulting contact areas are very small and the resulting pressures very high. The stresses on those contact surfaces can be determined from analytical formulas.

## 3.7. HERTZIAN CONTACT THEORY

Wheel/rail contact phenomena results in stick slip wear, giving rise to crack initiation and its propagation to yield catastrophe. The contact condition in terms of contact pressure found to be more important than the grade of steel. Assessment of contact stresses at the wheel/rail interface thus poses a very important issue in a study of wheel/rail contact phenomena. It is important to understand here that wheel/rail contact pair's profile radii change with time and wear. This has drawn much attention of many researchers to investigate the problem mainly by means of theoretical or numerical approaches for the solution of Hertz theory [35]. Hertz contact theory appeared in 1881 to solve the problem of pressure distribution between two elastic spherical bodies in contact. Later he extended it to general case of two elastic bodies in contact. Then onwards researchers have used this theory for the analysis of the wheel/rail contact problem numerically to reach a more realistic solution. The contact-pair topology influences the contact stress magnitude and shape of contact area. Hertz theory has its own limitations in the assumptions. Hertz's model of contact stress relies on the following simplifying assumptions

- The materials in contact are homogeneous.
- Contact stress is caused by the load which is normal to the contact tangent plane, which implies that there are no tangential forces acting between the solids.
- The contact area is very small compared with the dimensions of the contacting solids.
- The contacting solids are at rest and in equilibrium.
- The effect of surface roughness is negligible

## 3.8. ANALYSIS OF LOAD DISTRIBUTION AND 3D CONTACT

If two elastic nonconforming bodies contact together then according to the Hertz contact theory, the contact area is elliptical in shape with a major semi-axis a and a minor semi-axis b [52].

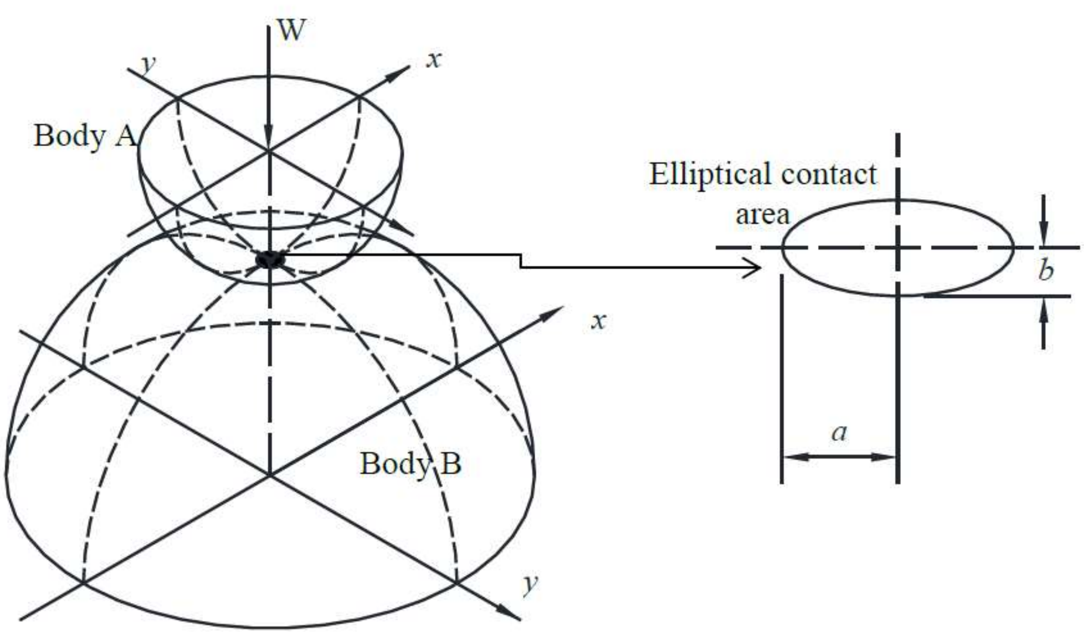


FIGURE 19: Geometry of two elastic bodies with convex surface in contact [52]

When considering two elastic bodies in contact, as shown in Figure 18.19 they will meet at a single point *O*, where the normal distance between them is zero. Near this contact point, without load, the body surface shapes may be represented by two second-order polynomials:

$$Z1=A1x^2+B1y^2 \quad 3.1$$

$$Z2=A2x^2+B2y^2 \quad 3.2$$

The coefficients A1, A2 and B1, B2are assumed to be constant.

The general conditions considered during the wheel rail contact simulation are the assumption of the Hertz contact theory. As explained in the previous chapter the common Hertz assumptions are:

- Isotropic and homogenous material
- No friction (The surfaces of both bodies had to be completely smooth)
- Both bodies were considered as half-spaces
- The contact is elastic.

In the case of a railway, the four main curvatures can be considered to be in perpendicular planes. Their directions correspond to the main axes of the frame: O-xy.

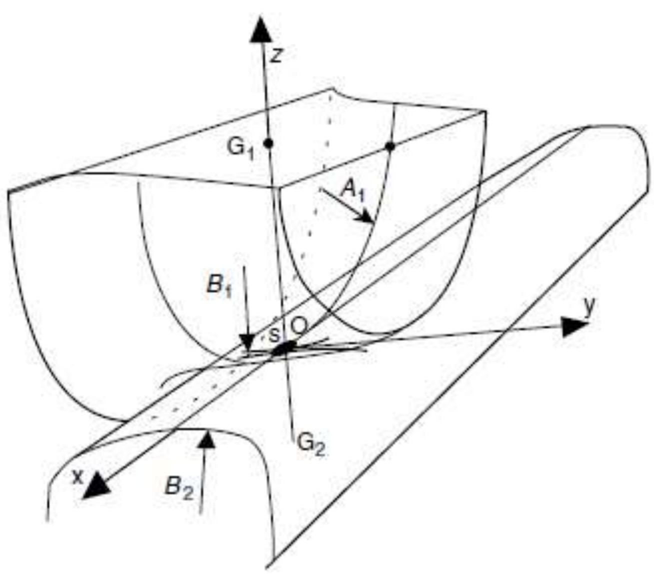


FIGURE 20: Hertzian contact: the Railway case [52].

In the 3D railway case, the above-mentioned curvatures and radii will be:

**Wheel: $d^2Z1/dx^2 = 2A1 = 1/R1w$** **3.3**

**Wheel: $d^2Z1/dy^2 = 2B1 = 1/R2w$** **3.4**

**Rail: $d^2Z2/dy^2 = 2B2 = 1/R2r$** **3.5**

Where $R1$w is the longitudinal radius of the wheel at the contact point, $R2w$ is the transversal radius of the wheel profile and $R2r$ is the transversal radius of the rail profile. In the railway case, the curvature $A2$ is generally neglected as the rail principal rolling radius $R1r$ is ∞.

According to Hertzian contact theory, the contact area of a wheel and rail is elliptical in shape, with the major and minor semi-axis $a$ and $b$ respectively (Figure 17). The contact pressure distribution $P$ in this area can be expressed as:

$$\mathbf{P} = \frac{3Fn}{2\pi ab} = \sqrt{1 - \left(\frac{x}{a}\right)^2 - \left(\frac{y}{b}\right)^2} \qquad \mathbf{3.6}$$

Where, $Fn$ is the applied normal load at the contact, a and b are semi axes of the contact ellipse, the magnitudes of $a$ and $b$ depend on the normal load, wheel and rail profiles and materials. X and Y are the required coordinates to specify the point of contacts on the rail surface based on the lateral rail surface parameter.

The contact ellipse semi-axes a and b are determined as follows:

$$\mathbf{a = m} \left[\frac{3\pi Fn(Kw+Kr)}{4K3}\right]^{1/3} \qquad \mathbf{3.7}$$

$$\mathbf{b = n} \left[\frac{3\pi Fn(Kw+Kr)}{4K3}\right]^{1/3} \qquad \mathbf{3.8}$$

According to these assumptions and by using equation (3.6) the maximum contact pressure, P0 (Hertz stress) occur at x=0 and y=0

$$\mathbf{P = Po} = \frac{3Fn}{2\pi ab} \qquad \mathbf{3.9}$$

Depending on the size and orientation of the contact ellipse the positions of the contact point may be shifted in different directions based on the magnitude of x or y. However, based on the above general Hertz contact formula and assumptions, the stress due to wheel/rail contact decreases and becomes zero if it goes far away from the centerline of the rail head. Similarly, the wheel/rail contact stress is inversely proportional to the major and minor axis of the contact ellipse. To calculate a and b, first let's find the values of $Kw$, $Kr$ and $K3$. $Kw$ And $Kr$ are constants that depend on the material properties of railway wheel and rail respectively.

**Where** $\quad Kw = \frac{1-(vw)^2}{\pi Ew}$ **3.10**

**And** $\quad Kr = \frac{1-(vr)^2}{\pi Er}$ **3.11**

Where $vw$ and $Ew$ are Poisson's ratio and young's modulus of the railway wheel material and $vr$, and $Er$ are Poisson's ratio and young's modulus of railway rail material.

$$Kw = \frac{1-(0.3)^2}{\pi \times 210 \times 109} = \quad Kw = 1.38\times10-12 \ \mathbf{m^2/N}$$

**Also**

$$Kr = \frac{1-(0.3)^2}{\pi \times 207 \times 109} = \quad Kr = 1.4\times10-12 \ \mathbf{m^2/N}$$

$K3$ is a constant and depends on the geometric properties of the two bodies and is defined as follows

$$K3 = \frac{1}{2}\left(\frac{1}{R1w} + \frac{1}{R2w} + \frac{1}{R1r} + \frac{1}{R2r}\right) \qquad 3.12$$

$R1$w and $R1$r, are the Principal rolling radii of the wheel and the rail respectively and $R2$w $a$nd $R2$r, are the principal transverse radii of curvature of the wheel and rail respectively.

$$K3 = \frac{1}{2}\left(\frac{1}{330} + \frac{1}{\infty} + \frac{1}{\infty} + \frac{1}{300}\right) = 0.0032 \ mm^{-1}$$

The coefficients m and n are Hertz coefficients and they are given as a function of the angle $\theta$ (45− 90) where $\theta$ is defined as:

$$\theta = \cos{-1}\left(\frac{K4}{K3}\right) \qquad 3.13$$

$$\text{Where } K4 = \frac{1}{2}\sqrt{\left(\frac{1}{R1w} - \frac{1}{R2w}\right)^2 + \left(\frac{1}{R1r} - \frac{1}{R2r}\right)^2 + 2\left(\frac{1}{R1w} - \frac{1}{R2w}\right)\left(\frac{1}{R1r} - \frac{1}{R2r}\right)cos2\emptyset} \qquad 3.14$$

$\varphi$ Is the angle of the orientation difference of the principle axes of the two bodies; also called yaw rotation. For a straight segment the curvature of the rail, φ=45˚ Therefore,

$$K4 = \frac{1}{2}\sqrt{\left(\frac{1}{330} - \frac{1}{\infty}\right)^2 + \left(\frac{1}{\infty} - \frac{1}{300}\right)^2 + 2\left(\frac{1}{330} - \frac{1}{\infty}\right)\left(\frac{1}{\infty} - \frac{1}{300}\right)cos2(45^\circ)}$$

**K4 = 0.00225 mm$^{-1}$**

For a straight rail-Wheel contact, $\theta$ is defined as:

$\boldsymbol{\theta} = \mathbf{cos}{-}\mathbf{1}\ (\frac{k4}{k3})$ **3.15**

$\boldsymbol{\theta} = \mathbf{cos\text{-}1}\ (\frac{0.0025}{0.0032})$

$\boldsymbol{\theta}$ = **45.3 °**

By using the Hertz coefficient table and linear interpolation method the value of m and n for the selected rail can be easily obtained.

**Table 14: Hertz coefficients**

| θ (deg) | m | n | θ (deg) | m | n | θ (deg) | m | n |
|---|---|---|---|---|---|---|---|---|
| 0.5 | 61.4 | 0.1018 | 10 | 6.6 | 0.311 | 60 | 1.49 | 0.72 |
| 1 | 36.89 | 0.1314 | 20 | 3.81 | 0.413 | 65 | 1.38 | 0.76 |
| 1.5 | 27.48 | 0.1522 | 30 | 2.73 | 0.493 | 70 | 1.28 | 0.8 |
| 2 | 22.26 | 0.1691 | 35 | 2.4 | 0.53 | 75 | 1.2 | 0.85 |
| 3 | 16.5 | 0.1964 | 40 | 2.14 | 0.567 | 80 | 1.13 | 0.89 |
| 4 | 13.31 | 0.2188 | 45 | 1.93 | 0.604 | 85 | 1.06 | 0.94 |
| 6 | 9.79 | 0.2552 | 50 | 1.75 | 0.641 | 90 | 1 | 1 |
| 8 | 7.86 | 0.285 | 55 | 1.61 | 0.678 | | | |

By interpolation method, we can calculate m and n

$\theta 1$=45°, m1=1.93, n1= 0.604, $\theta 2$=90° m2= 1, n2= 1

$\boldsymbol{m} = \mathbf{m1} + \frac{\mathbf{m2 - m1}}{\boldsymbol{\theta}\mathbf{2} - \boldsymbol{\theta}\mathbf{1}}\ (\boldsymbol{\theta} - \boldsymbol{\theta}\mathbf{1})$ **3.16**

$\boldsymbol{m} = \mathbf{1.93} + \frac{\mathbf{1-1.93}}{\mathbf{90-85}}\ \mathbf{(45.3\text{-}45)}$

$\boldsymbol{m}$ = **1.9238**

Similarly,

$n = n1 + \frac{n2-n1}{\theta2-\theta1}(\theta - \theta1)$ **3.17**

$n = 0.604 + \frac{1-0.604}{90-85}(45.3-45)$

$n =$ **<u>0.6066</u>**

- Tram car weight = **44 tones**

So the force **N = 44*10^3 * 9.81= 431640 N**

- Tram car weight on each wheel **= 44*10^3 /6= 7333.33 Kg**
- Carrying capacity **= 60 kg / person *318 = 19080 Kg**

Carrying capacity on each wheel **= 109080/6 = 3180 Kg**

- Overall capacity **= (7333.33+3180)* 9.81 =103135.473 N = 103.135473 Kg**

And, the axle load is ≤ 11(1+3%) tones.

Axle Load = (11+0.33) tones = 11330 kg.

The normal load (force) applied on each wheel is half of the axle load multiplied by the gravitational acceleration, that is:

$N = \frac{axle\ load \times g}{2} = \frac{11330 \times 10}{2}$ **3.18**

**N = <u>56650 N</u>**

Then the values of a and b are:

$a = m \left[\frac{3\pi Fn(Kw+Kr)}{4K3}\right]^{1/3}$ **3.19**

**a = 0.0094 m**

$b = n \left[\frac{3\pi Fn(Kw+Kr)}{4K3}\right]^{1/3}$ **3.20**

**b = <u>0.0030 m</u>**

By using the values of a, b and the normal force, the maximum Hertz contact stress will be:

$P = P0 = \frac{3Fn}{2\pi \times ab} = \frac{3 \times 56650}{2\pi \times 0.0094 \times 0.0030}$ **3.21**

**P = <u>958.3 Mpa</u>**

The maximum contact pressure of 958.3 Mpa is less than the ultimate tensile strength of wheel 2 (Bainitic) and more than the ultimate tensile strength of Wheel 1 (R7) therefore we can suppose that the Wheel 2 is more resistible than Wheel 1

The Angular velocity or Rotational velocity of the wheel with maximum operating speed of the vehicle is:

**W=** $\frac{v}{R1w}$ **3.22**

Where $v$ is the maximum operation speed of the vehicle, 70km/hr =19.44 m/s and $R1w$ is the principal rolling radius of the wheel, 330mm = 0.33m

**W =** $\frac{19.44}{0.33}$ **=** **<u>58.91 rad / s</u>**

**And the acceleration a = 1470mm / s²**

# CHAPTER FOUR: RESULT AND DISCUSSION

## 4.1. MODELING AND SIMULATION

In order to build a realistic model of wheel/rail contact problem a 3D elastic-plastic finite element model is needed. This model should be able to accurately calculate the 3D stress response in the contact region as well as includes both material and geometric nonlinearity. The model is constructed by CATIA V5 R16 software and imported to ANSYS 16.0 Workbench

The procedure of the simulation analyses is summarized below:

a) The models for wheel and rail are generated in CATIA. Then, after assembling the model in CATIA is imported in to ANSYS Workbench as working model.
b) Modules for automatic generation of finite element models are integrated into the model in ANSYS Workbench version 16.0, static structural analysis system. Then, the generation of finite element models is accomplished for the cycle of meshing.
c) Define material properties which are necessary to solve the problem. Here both the wheels and rail are R7 steel with an ultimate tensile strength of 820MPa, yield strength 840MPa. Young's modulus of elasticity is 210 GPA for existing one and for the new wheel rail material are Bainitic with ultimate tensile strenght of 1090 Mpa , yield strenght 860 Mpa , Young's modulus of elasticity is 210 GPA for new one
d) Defining the fixed support and the applied force (pressure)
e) Finally, we can get solution

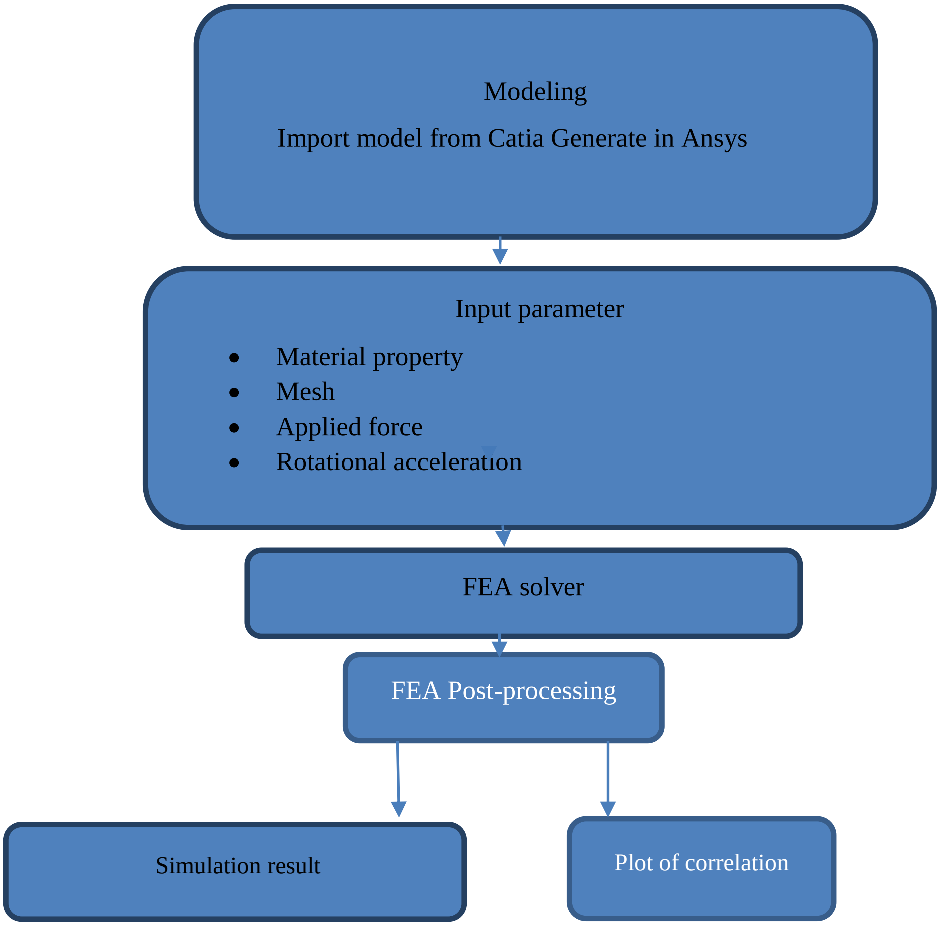


Figure 21: Modeling and simulation

## 4.2. WHEEL AND RAIL CONTACT MODELING (CATIA)

Before performing any type of analysis, the solid modeling of the material is mandatory using solid modeling software the 3D model of the railway wheel and rail is created using the CATIA V5 software package. The modeled wheel and rail used in the analysis is the same for different case. Because the wheels are different in material composition and properties, not in structural dimension

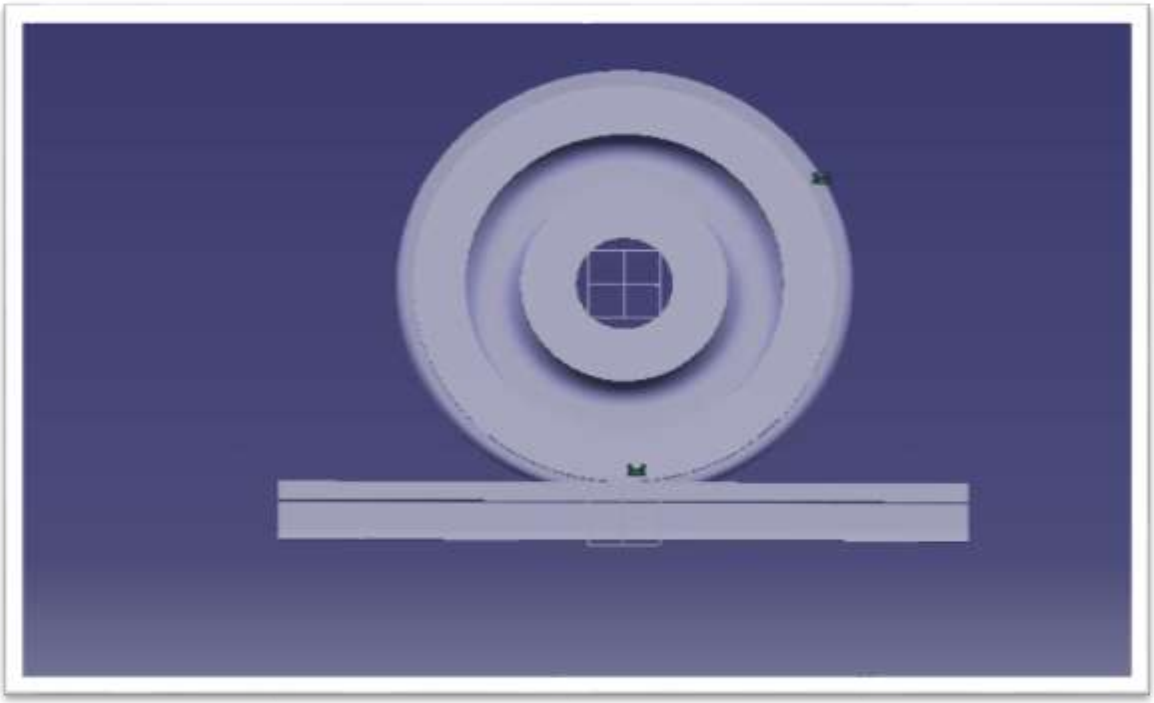

Figure 22: Wheel/rail contact model with CATIA

## 4.3. FINITE ELEMENT ANALYSIS

The finite element analysis (FEA) is a computing technique that is used to obtain approximate solutions to boundary value problems. It uses a numerical method called finite element method (FEM). FEA involves the computer model of a design that is loaded and analyzed for specific results, such as stress, deformation, deflection, natural frequencies, mode shapes, temperature distributions, and so on. The railway track was modelled and analyzed using the finite element software ANSYS 16

### 4.3.1. IMPORTING THE FILE FROM CATIA

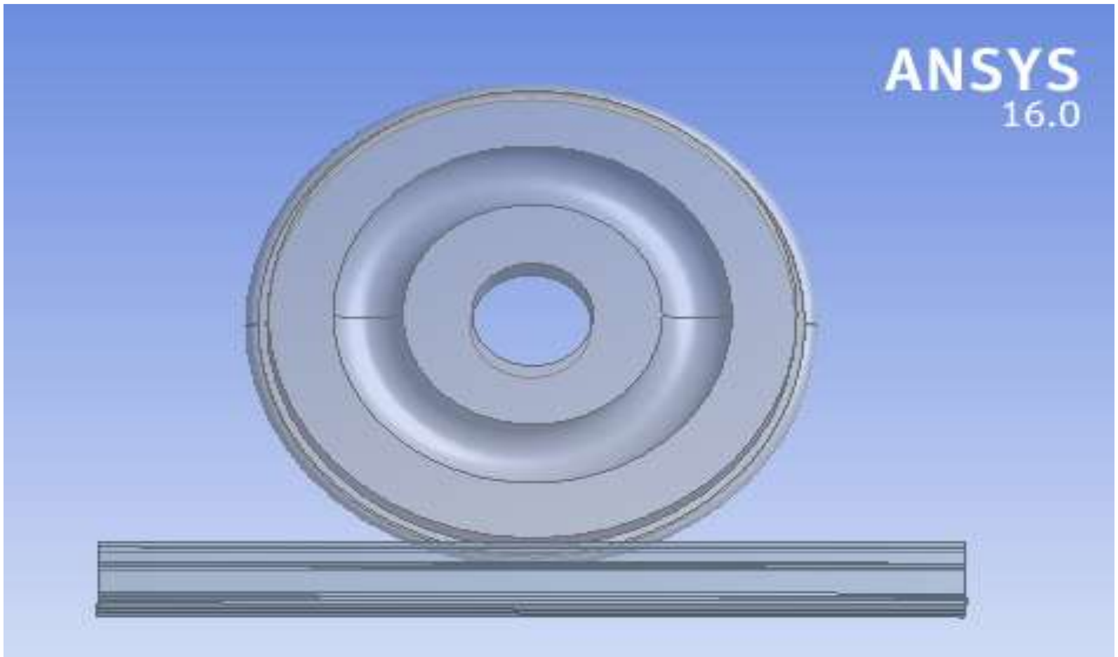


Figure 23: Wheel/rail contact model imported to ANSYS

## 4.4. MESHING

Meshing is discretizing the solid object to finest parts to perform the analysis to get the precise value at each and every element of the meshed object. To get value that approximated to actual value this model used fine meshed method

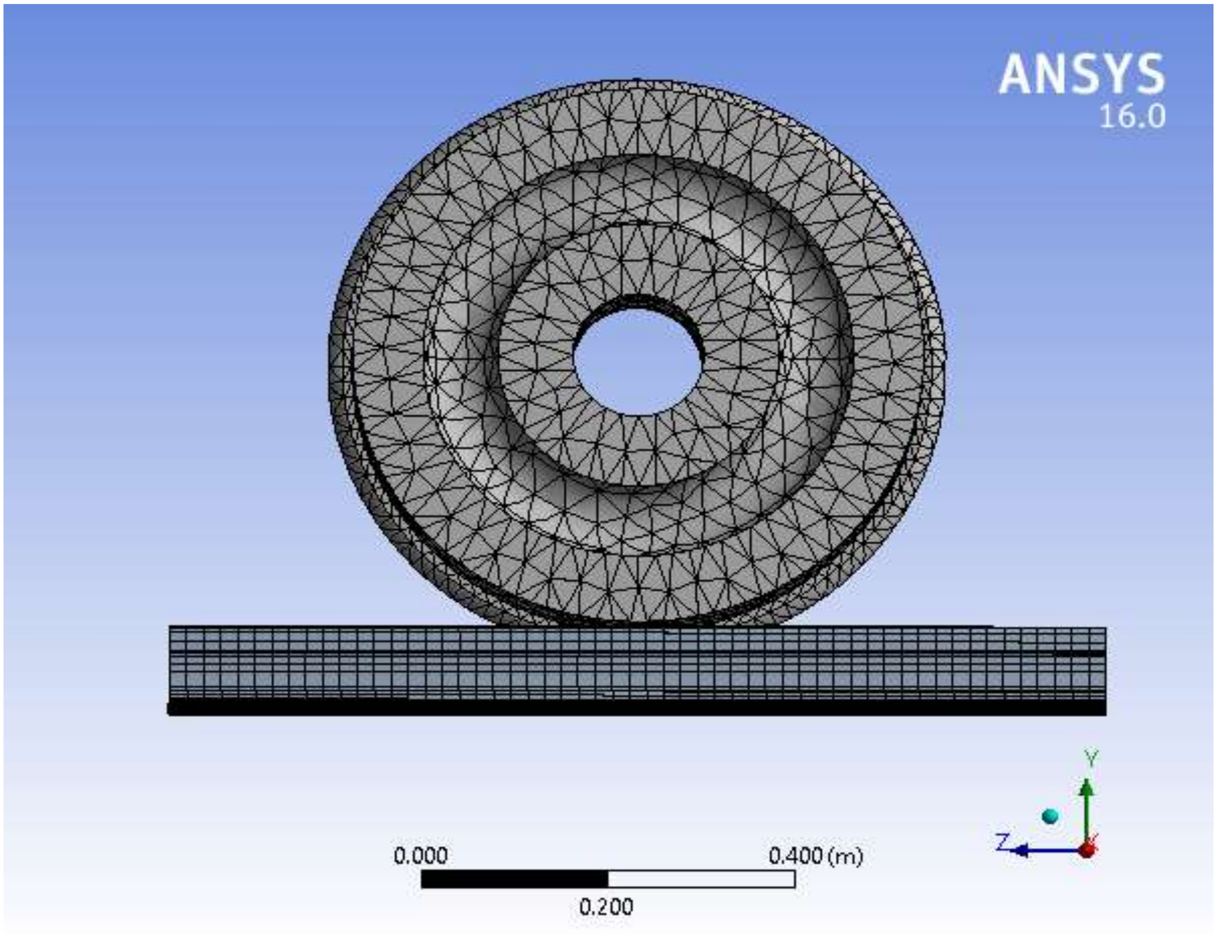


Figure 24**:** Meshed models of the wheel –rail contact

Fixed boundary condition is applied to the rail at the bottom of the foot. Force is applied on the wheel and the rotational velocity of the wheel is applied to the wheel center. Also, the standard earth gravity is applied.

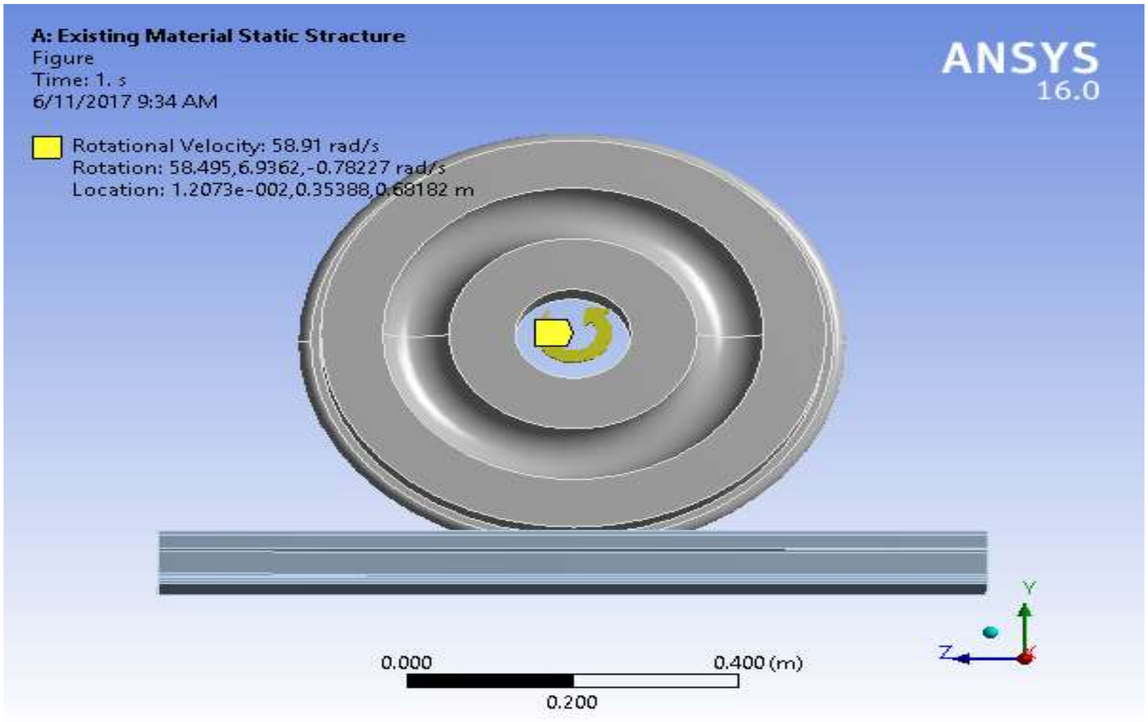


Figure 25**:** Rotational velocity models of the wheel –rail contact

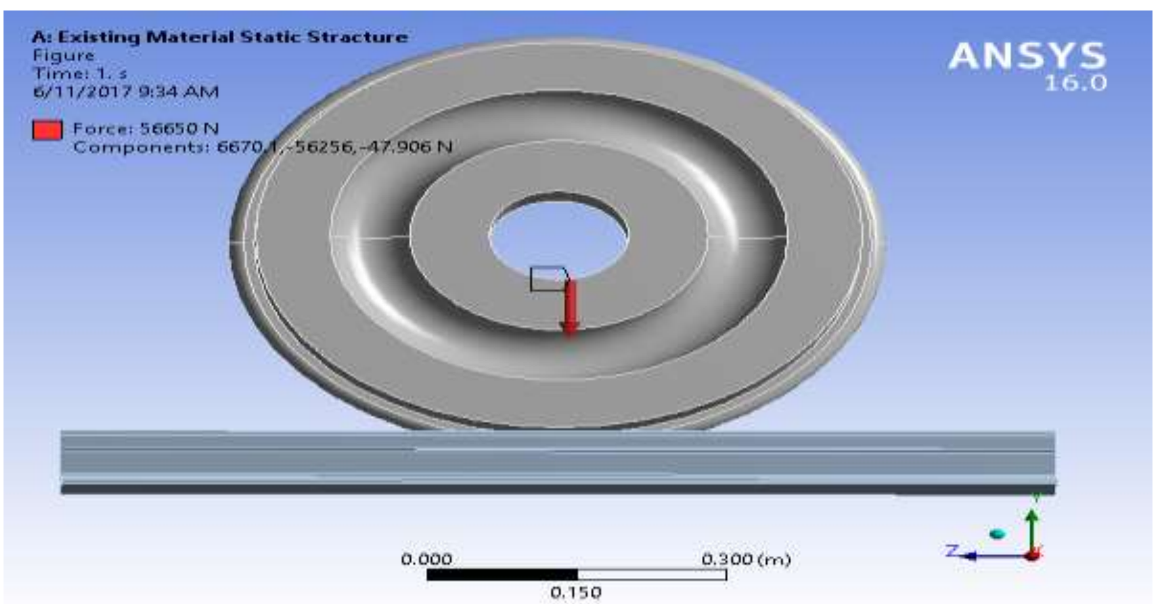


Figure 26**:** Load apply models of the wheel –rail contact

## 4.5. RESULTS STATIC ANALYSIS

In this part, the result of stress analysis and the contact pressure from the finite element model under different material properties will be discussed in details. Figures below show the stress Analysis on the contact between Wheel/rail

### 4.5.1. EQUIVALENT VON-MISES STRESS

The figures (figure 27 and 28) demonstrate the (von-Mises) stress distribution on wheel and rail contact for Wheel 1 (336 Mpa maximum and 0.008907 Mpa minimum values) and Wheel 2 (255 Mpa maximum and 0.016308 Mpa minimum values) the contact between Wheel and Rail has the maximum stress

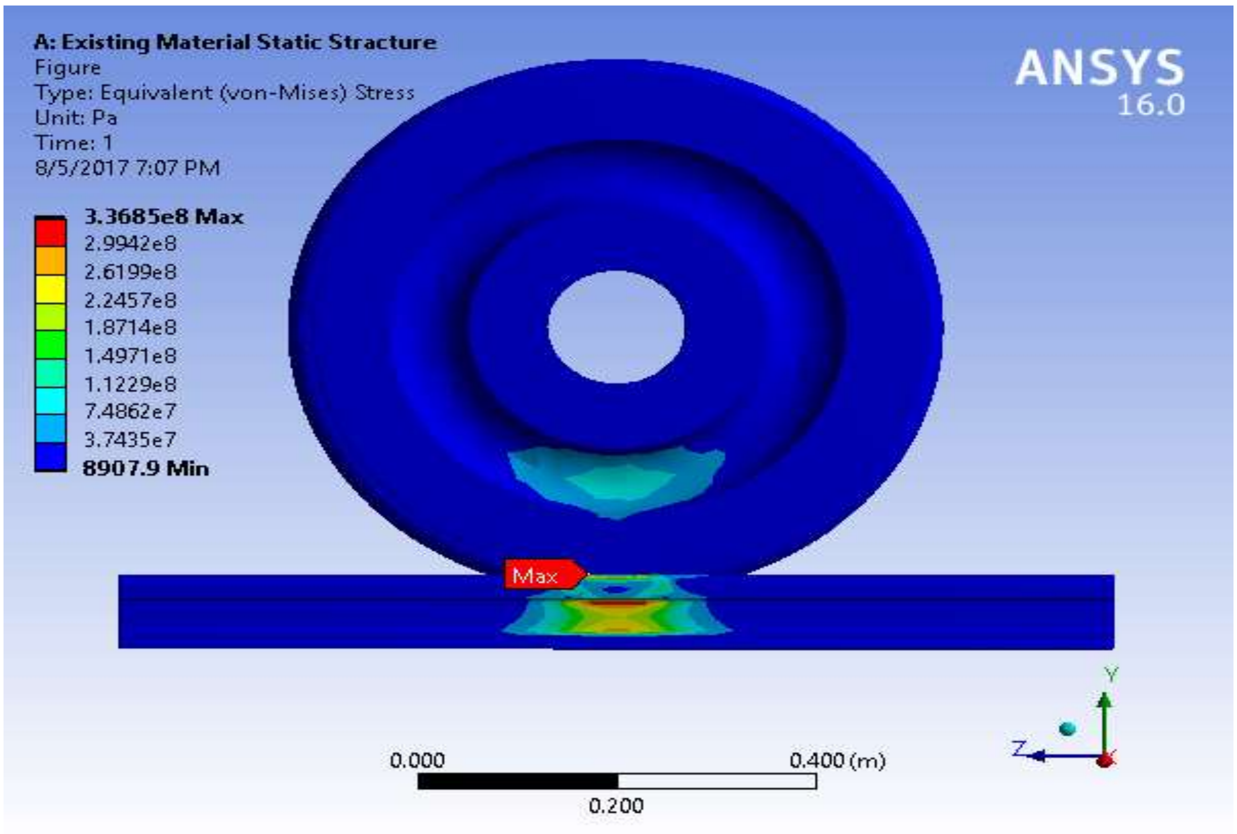


Figure 27: Von-Mises stress on wheel 1

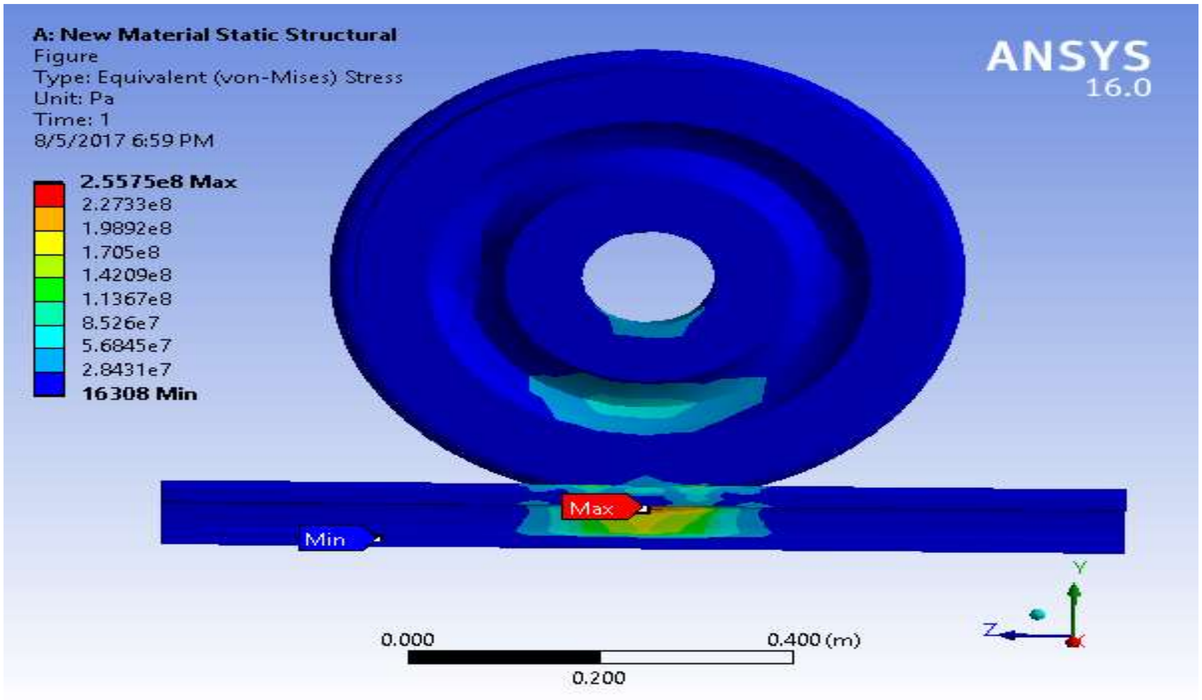


Figure 28: Von-Mises stress on wheel 2

### 4.5.2 EQUIVALENT ELASTIC STRAIN

The next figures demonstrate the equivalent elastic strain distribution on wheel-rail contact (29 and 30) below, the equivalent elastic strain on wheel 1 (1.97 x 10-3 maximum and 5.63 x 10-8 minimum values) and wheel 2 (1.2234 x 10-3 maximum and 9.44 x 10-8 minimum values) are build.

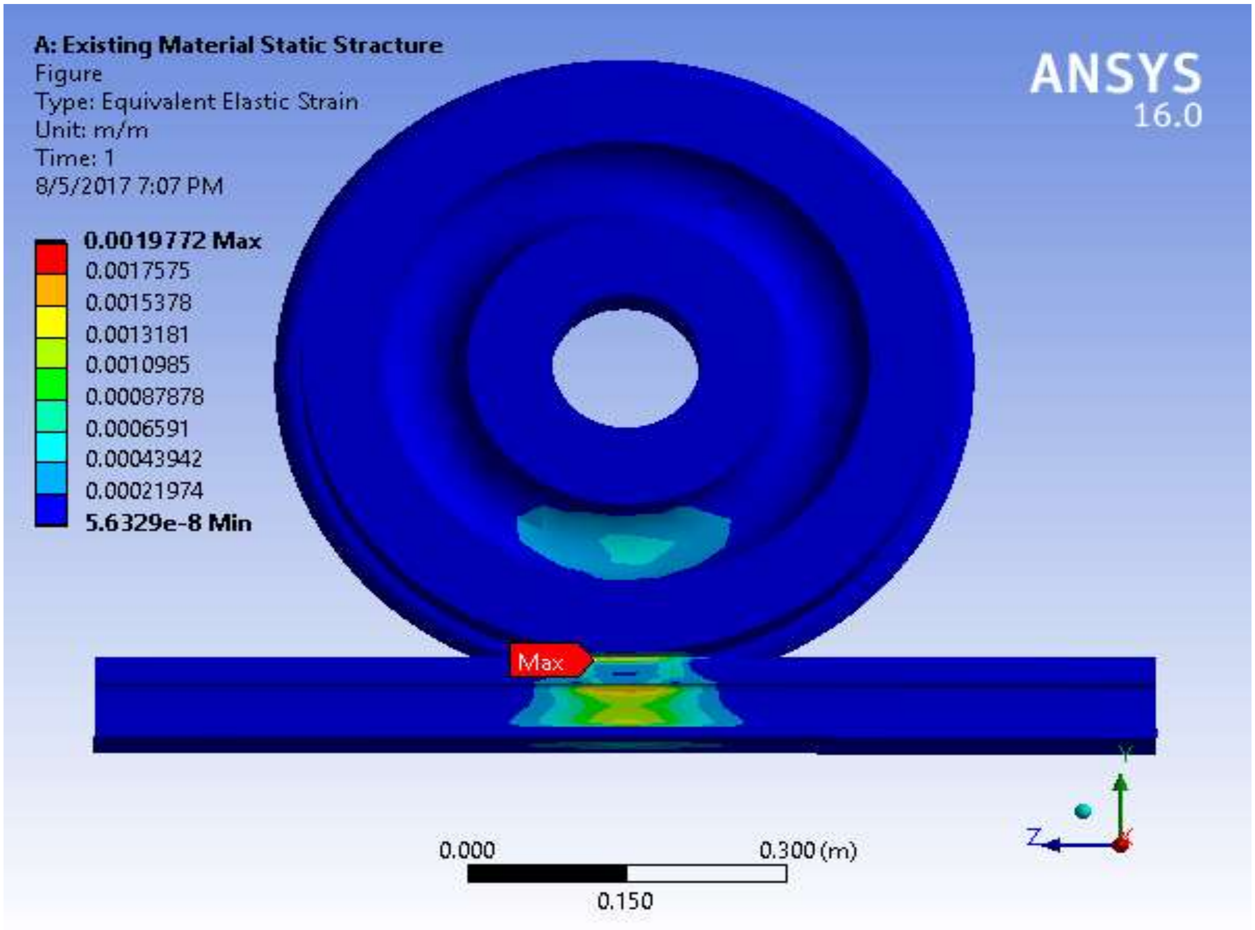


Figure 29: Equivalent Elastic Strain on wheel 1

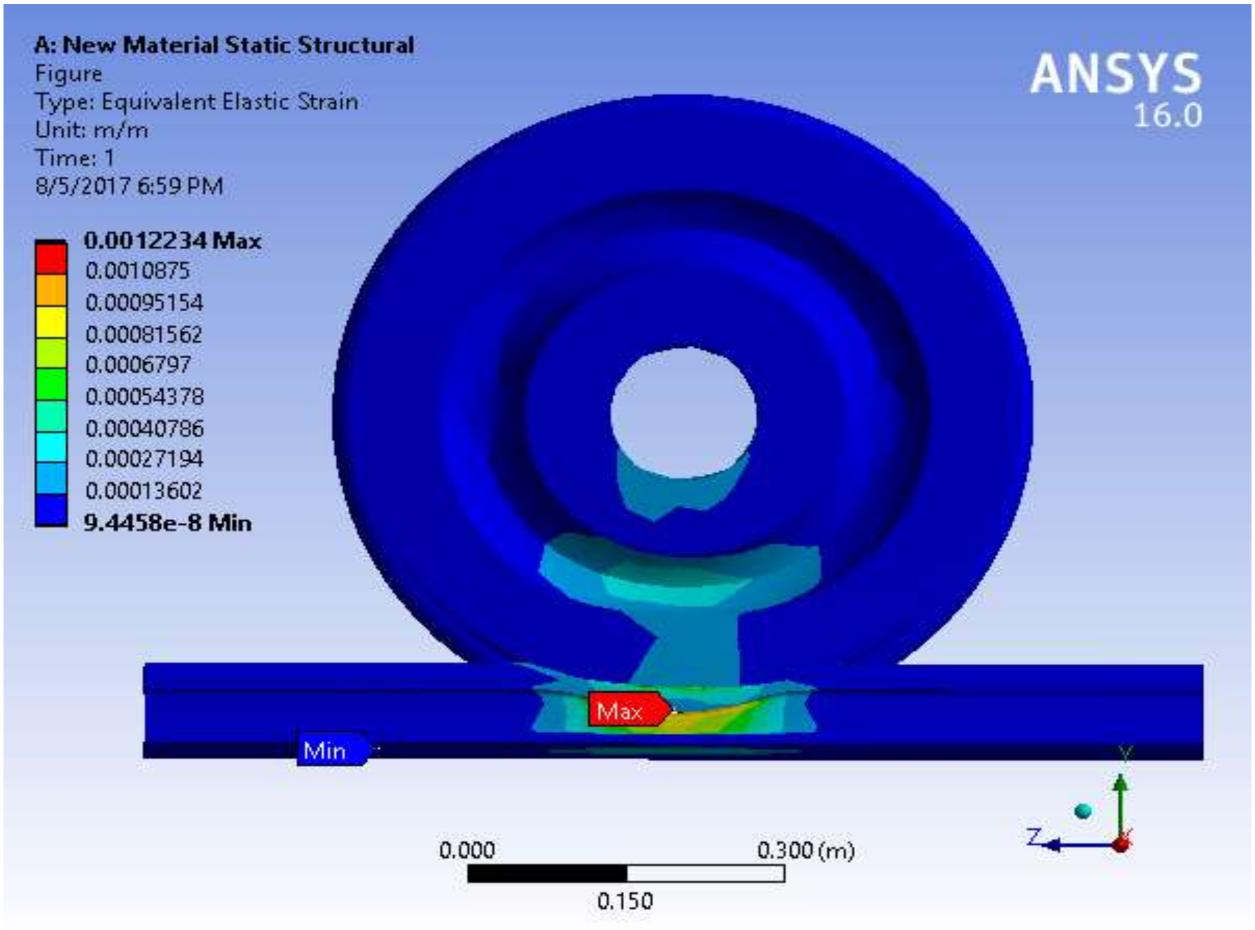


Figure 30: Equivalent Elastic Strain on wheel 2

## 4.5.3. MAXIMUM SHEAR ELASTIC STRAIN

In the figures (31 and 32) below, the maximum shear elastic strain on wheel 1 (2.49 x 10-3 maximum and 6.67 x 10-8 minimum values) and wheel 2 (1.715 x 10-3 maximum and 1.1271 x 10-7 minimum values) are build.

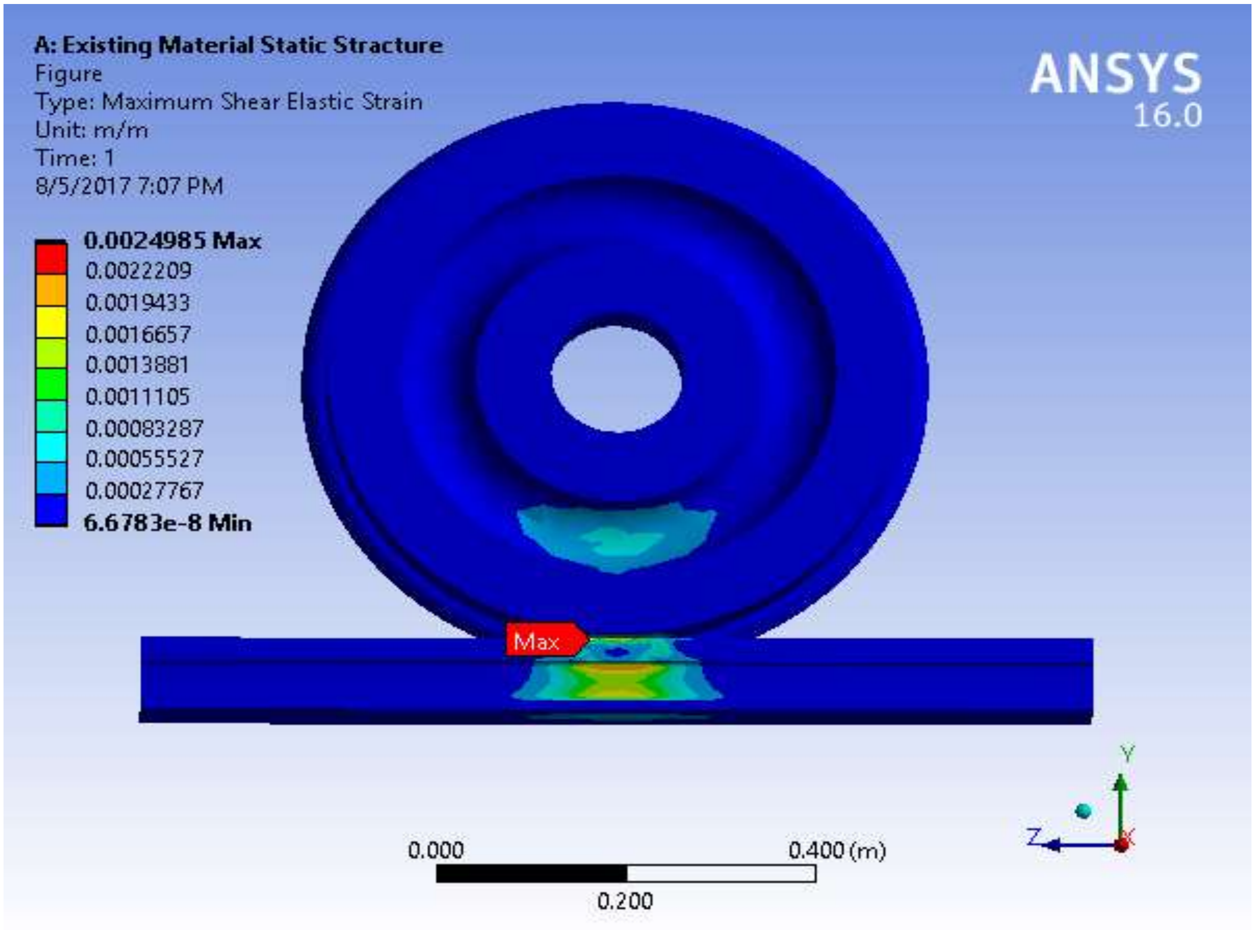


Figure 31: Maximum shear Elastic Strain on wheel 1

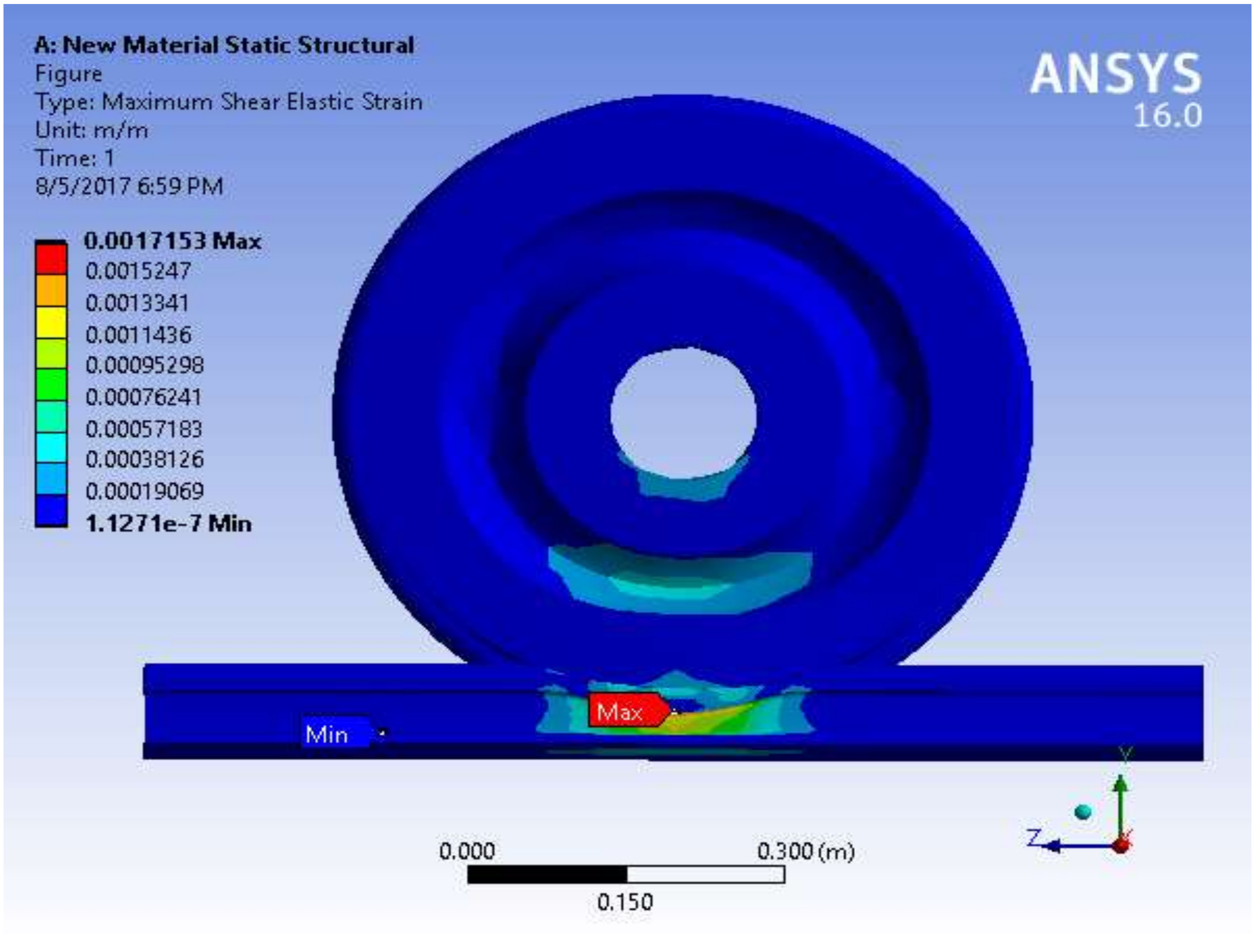


Figure 32: Maximum shear Elastic Strain on wheel 2

## 4.6. DISCUSSION

A finite element analysis model was developed in order to investigate all the variations of the contact force, (Von-Mises) stress, equivalent elastic strain, Maximum shear elastic strain and pressure between the wheel and the rail contact at different materials was discussed in this section

**Table 15:** Discussion of wheel and rail contact material

| Wheel and Rail contact | R7and UIC 50 | Bainitic and UIC 50 |
|---|---|---|
| Rotational velocity(rad/s) | 58.91 | 58.91 |
| Force apply | 56650 | 56650 |
| Von-Mises stress (Mpa) | 336 | 255 |
| Equivalent Elastic strain | 1.977 x 10-3 | 1.22 x 10-3 |
| Maximum Shear Elastic Stain | 2.49 x 10-3 | 1.715 x 10-3 |

The pressure produced for the two-different pair of the wheel and rail material (R7 and UIC 50), (BAINITIC and UIC 50) were compared to each other.

Among the investigated materials, the pair (BAINITIC and UIC 50) show less value the stress this is because of the composition of the wheel material (increasing the carbon content in the material and also increasing the hardness improve the ductility and wear resistance of the material)

The wheel and rail contact (Von-Mises) stress and equivalent elastic strain have been performed for different materials using the analysis SOFTWARE "ANSYS "the result were obtained from the simulation show as that the wheel 2 has low stress and equivalent elastic strain then wheel 1 and the result approved the performance of this material

**V =K $\frac{NS}{H}$**

❖ **For the wheel 1 ( R7)**

- the hardness H=241 HB
- K = 7*10^ ⁻ ³
- S =V*t = 3500 m
- N = P*A where A = a*b*π = 0.0094*0.0030*π =8.86*10^⁻ 5

❖ **For the wheel 2 ( Bainitic)**

- The hardness H =273 HB
- K = 7*10^ ⁻ ³
- S =V*T = 3500 m
- N = P*A where A = a*b*π = 0.0094*0.0030*π =8.86*10^⁻ 5

Table14: Wear volume of wheel 1 and wheel 2

| Pressure (Mpa) | Wear Volume 1 | Wear Volume 2 |
|---|---|---|
| 500 | 4.50E-03 | 3.90E-03 |
| 600 | 5.40E-03 | 4.70E-03 |
| 700 | 6.30E-03 | 5.56E-03 |
| 800 | 7.20E-03 | 6.30E-03 |
| 820 | 7.30E-03 | 6.50E-03 |
| 900 | 8.10E-03 | 7.10E-03 |
| 1000 | 9.00E-03 | 7.90E-03 |
| 1090 | 9.80E-03 | 8.60E-03 |
| 1100 | 9.90E-03 | 8.70E-03 |

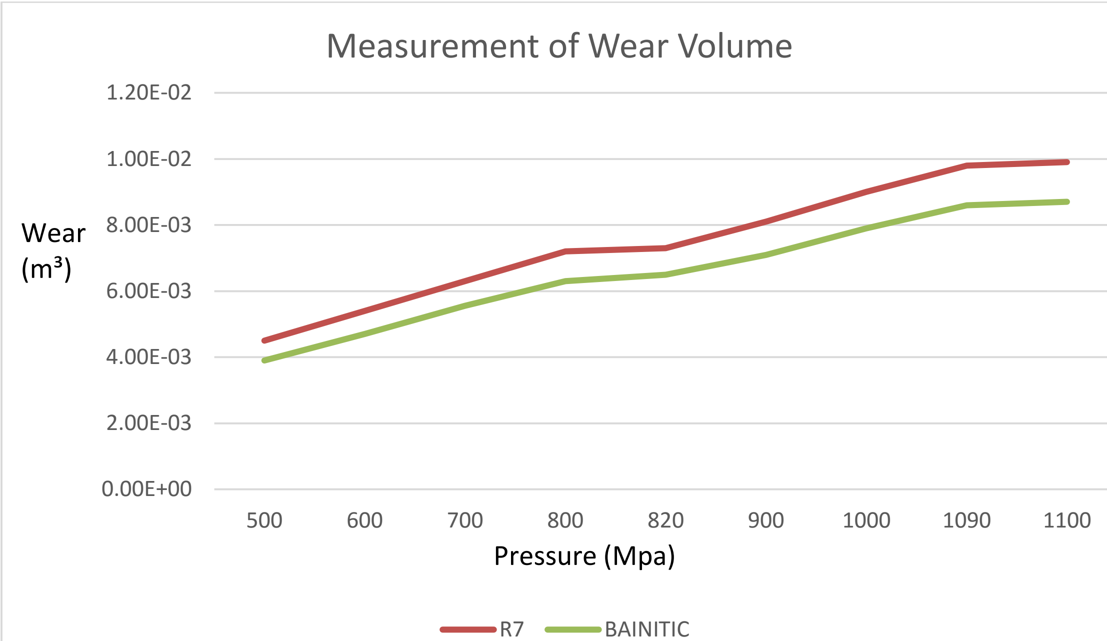


Figure 33: The graph of wear measurement

In the graph above, the wear volume and the pressure are given for two different wheels the result shows that the wear volume on wheel-rail contact increases with increasing pressure.

Even though the wear volume increase for each wheel-rail contact, the wear volume on wheel 1 is greater than the wear volume on wheel 2.

This proves that wheel 2 material has better strength and hardness then wheel 1, this is because of the material composition difference and physical properties

# CHAPTER FIVE: CONCLUSION AND RECOMANDATION AND FUTUR WORK

## 5.1. CONCLUSION

In this research, the wear analysis on wheel-rail contact in rolling and sliding contact is studies. During rolling-sliding contact there is stress produced between wheel-rail contact, this stress is applied on wheel 1 (R7) and wheel 2 (BAINITIC) which have different chemical composition and property, but same structural dimension.

From the present work, which investigates the effect of different wheel material the conclusions may be drawn as the following: -

- The wheels are analyzed by ANSYS and the result obtained is that wheel 2 (BAINITIC) is better in resisting wear because of its improved chemical composition and material properties.

- Wheel 2 (BAINITE) steel may provide improved performance and minimize the wear and can provide longer life

## 5.2. RECOMMENDATION

As it is said and analyzed before, the wheel 2 (Bainitic) material compositions is enhanced than that of wheel 1 (R7). So, it’s better for Ethiopian Railway Corporation to use this wheel (Wheel 2) for Addis Ababa Light Railway Transit by making further study.

## 5.3. FUTURE WORK

The following are suggested for future work as extensions and elaborations of this Research.

- More investigation of wheel materials with experimental analysis
- Additional study by considering vertical and horizontal loads.
- Influences different environmental contact (dry, wet, and oily) on wheel/rail

## REFERECES


[1] Z. Li. Wheel-Rail Contact and Its Application to Wear Simulation. Doctoral Thesis proposal, Delft university of Technology, (2002). ISBN 90-407-2281-1.

[2] R. Enblom. On simulation of uniform wear and profile evolution in the wheel-rail contact, Doctoral Thesis KTH, Stockholm, Sweden (2006).

[3] R. Roberti, S. Bruni. Development of operations of tilting train on Italian network, Proceedings 5th World Congress on Railway Research, Koln, Germany, 25-29, (2001).

[4] J.A. Williams, *Wear modelling, analytical, computing and mapping: a continuum mechanics approach.* Wear, 225–229 (1999) pp. 1–17.

[5] Rail profile Wikipedia

[6] Filonov S.P., Gibalov A.I., Nikitin E.A. and others. 2TE116 diesel locomotive. Edition 3rd, revised and enlarged. -M.: Transport, 1996. – 334p.

[7] Lukin V.V. and others. Designing and calculation of vehicles. -M.: TMD MR of Russia, 2000. 731p.

[8] Myamlin S.V., Kupriyan Y.O. Process approach to quality management at the car-repair plant // Railway transport of Ukraine. – 2006. -.6 -P. 50-52.

[9] F. Bucher, K. Knothe, and A. Theiler, Normal and tangential contact
Problem of surfaces with measured roughness (2002) (to appear in
Wear).

[10] B.N.J. Persson, F. Bucher, and B. Chiaia, Elastic Contact Between
Randomly Rough Surfaces: Comparison of Theory with (Exact) Numerical
Results (2001) (to appear in J. Chem. Phys.).

[11] F.de C. Santos: "*Evaluation of subsurface contact stresses in rail road wheels using an elastic half-space model Elsevier, (2004) pages 420-429.*

[12] Xuesong Jin, Xinbiao Xiao, Zefeng Wen, Jun Guo, Minhao Zhu-" *An investigation into the effect of train curving on wear and contact stresses of wheel and rail", Elsevier, Tribology International 42 (2009) pages 475–490.*

[13] H.M. Tournay – "*A future challenge to wheel/rail interaction analysis and design: Predicting worn shapes and resulting damage modes", Elsevier, Wear 265 (2008) pages 1259–1265*

[14] M. Wiesta, E. Kassa, W.Daves- "*Assessment of methods for calculating contact pressure in wheel-rail/switch contact", Elsevier, Wear 265 (2008) pages 1439–1445.*

[15] Roya Sadat Ashoftech**:** *Calculating the contact stress resulting from lateral movement of the wheel on rail by applying Hertz theory (2013) pages 148–154.*

[16] Juraj Gerlici, Tomas Lack-*"Contact geometry influence on the rail / wheel surface stress distribution", Elsevier, Procedia Engineering 2 (2010) pages 2249–2257.*

[17] N. Bosso: "*Review of wheel- contact models" (2013) pages 5-19*

[18] Yi Zhu, Ulf Olofsson, Anders S¨ oderberg –"Adhesion *modelling in the wheel–rail contact under dry and lubricated conditions using measured 3D surfaces",SciVerse Science Direct, Tribology International 61 (2013) pages 1 10.*

[19] D. Milkovic, G. Simic ,Jakovljevic, J. Tanaskovic , V. Luc ˇanin-*" Wayside system for wheel–rail contact forces measurements", Elsevier, Measurement 46 (2013) pages 3308–3318.*

[20] Fujie Xia, Colin Cole, Peter Wolfs – "*The dynamic wheel –rail contact stresses for wagon on various tracks", Elsvier, Wear 265(2008) 1549-1555*

[21] W Yan, F.D. Fiscer- "*Applicability of Hertz contact theory to rail wheel contact problems", Archieve of applied mechanics 70(2000) 255-268*

[22] http://www.iitk.ac.in/infocell/iitk/newhtml/storyoftheweek60.htm

[23] Stanca, M., Stefani, A., Gallo, R., "Development of an Integrated Design Methodology for a New Generation of High Performance Rail Wheel sets", Proceedings of the 16th European MDI User Conference, Berchtesgaden, Germany, 14-15 November 2001.

[24] Jendel, T., "Prediction of Wheel Profile Wear - Comparisons with Field Measurements", Proceedings of the International Conference on Contact Mechanics and Wear of Rail/Wheel Systems, Tokyo, Japan, 2000, pp117124.

[25] Fries, R.H., Davila, C.G., "Wheel Wear Predictions for Tangent Track Running", Transactions of the ASME, Journal of Dynamic Systems, Measurement, and Control, Vol. 109, 1987, pp397-404.

[26] Pearce T.G., Sherratt N.D., "Prediction of Wheel Profile Wear", Wear, Vol. 144, 1991, pp343-351.

[27] Zobory, I. “Prediction of Wheel/Rail Profile Wear”, Vehicle System Dynamics, Vol. 28, 1997, pp221-259.

[28] Lewis, R., Dwyer-Joyce, R.S., Bruni, S., Ekberg, A., Cavalletti, M., Bel Knani, K., “A New CAE Procedure for Railway Wheel Tribological Design”, accepted for presentation at the 14th International Wheelset Congress, Florida, $17^{th}$ 21st October 2004.

[29] Telliskivi T., Olofsson U., “Contact mechanics analysis of measured wheel-rail profiles using the Finite Element Method”, Journal of Rail and Rapid Transit ,Proceedings of the IMechE, Part F, Vol. 215, 2001, pp65-72.

[30] Telliskivi T., Olofsson U., “Wheel-Rail Wear Simulation”, accepted for publication by Wear.

[31] Jendel, T., “Prediction of Wheel Profile Wear – Methodology and Verification”, Licentiate Thesis, TRITA-FKT 2000:9, Royal Institute of Technology, Stockholm, Sweden, 2000.

[32] D. I. Fletcher and J. H. Beynon (2000). Development of a machine for closely controlled rolling contact fatigue and wear testing. J. Test. Eval. 28(4), 267-275.

[33] Revisiting the Archard’s wear equation. Methods of data analysis for wear sliding tests.

A. Ramalho

[35]: ARTC, Rail Defects Handbook, Some Rail Defects their Characteristics Causes and Control, Engineering Practices Manual, 2006

[36]: Malcolm kerr, Rail Defect hand Book, Rail corp engineering manual-track, 2012

[37]: Xiangyuan Xu, Estimation of Stress Intensity Factor Ranges for Slant Crack under Cyclic Rolling Contact Fatigue, Sungkyunkwan University, 2010

[38]: Rail and rolled product for railway application, Luchini S.P.A., Headquarters, Berecia Italy, www.lucchini.com

[39]: Santamaria, J., Vadillo, E.G., Oyarzabal, Wheel-rail wear index prediction considering Multiple contacts patches. 2009, Vol. 267, pp. 1100-1104

[40]: Joao, Application of computational tools to study the influence of worn wheel on railway vehicle dynamics, 2012, pp.51-61

[41]: Pombo, J., Ambrosio, J., Pereira, M., Lewis, R., Dwyer-Joyce, R., Ariaudo, C., Kuka, N. A study on wear evaluation of railway wheels based on multibody dynamics and wear computation, Multibody System Dynamics, 2010, pp. 347-366

[42]: UIC CODE 5, Trailing stock: wheels and wheel-sets, 4th edition, 2004

[43]: Rail Corp Engineering Standard, “ESR 0330 Wheel Defect Manual.” Railcorp, May-2013.

[44]: M. Clarke, “Wheel rolling contact fatigue (RCF) and rim defects investigation to further knowledge of the causes of RCF and to determine control measures.” Rail Safety and Standards Board, 2008.

[45]: New wheel steel set to improve wear resistance

[46]: Matsumura, R., H. Sugiyama and Y. Suda (2011). Analysis of Vehicle/Turnout Interactions of Railroad Vehicles Using Multiple Contact Tables. Journal of System Design and Dynamics. 5:3.

[47]: Yan, W. and D. Fischer (2000). Applicability of the Hertz contact theory to rail-wheel Contact problems. Archive of Applied Mechanics. 70: 255-268.

[48]: (2012). History of Rail Transport. Wikipedia, the Free Encyclopedia. http://en.wikipedia.org/wiki/History_of_rail_transport. Accessed Date, 23-10-2012.

[49]: Material used for wheels on rolling stock by katrin Madler

[50]: Railway rolling stock materials — Part 3: Specification for monobloc wheels for traction and trailing stock

[51]: K. Mädler, A. Zoll, R. Heyder, M. Brehmer *Deutsche Bahn AG, DB System technik, Brandenburg-Kirchmöser, Germany*

[52] Munidasa Widhana, Investigation of Surface Ratchetting due to Rail/Wheel Contact, Doctoral thesis, 2013